

THE ROLE OF RESTING MAST CELLS IN THE SURVIVAL OF
MYENTERIC NEURONS

THE ROLE OF RESTING MAST CELLS IN THE SURVIVAL OF
MYENTERIC NEURONS IN A PRIMARY LONGITUDINAL
MUSCLE-MYENTERIC PLEXUS & BONE MARROW-DERIVED
MAST CELL CO-CULTURE SYSTEM

By JAIME KNOCH, H.BSc.

Submitted to the School of Graduate Studies in Partial Fulfilment of
the Requirements for the Degree Master of Science

McMaster University © Copyright by Jaime Knoch, September 2019

McMaster University MASTER OF SCIENCE (2019) Hamilton,
Ontario (Medical Science)

TITLE: The role of resting mast cells in the survival of myenteric
neurons in a primary longitudinal muscle-myenteric plexus & bone
marrow-derived mast cell co-culture system AUTHOR: Knoch,
H.BSc. (McMaster University) SUPERVISOR: Professor P. Forsythe
PAGES: vii, 60.

Lay Abstract

The enteric nervous system is a vast web of nerves and immune cells that innervates the gut and interacts with the central nervous system through the gut-brain axis. An important mediator in this system is the mast cell, a type of immune cell often involved in protective responses to venoms and allergens. Intriguingly, in normal physiological conditions these cells are in close contact with nerves in the periphery, despite their potential to release damaging constituents. While mast cells are well-known for inciting inflammation and releasing toxic granules, they can also synthesize and release potentially beneficial neuroactive compounds, such as neurotransmitters or growth factors. The aim of this study was to characterize mast cell-nerve interactions in neurotoxic conditions, to see if the proximity of mast cells to nerves might serve a neuroprotective purpose.

Abstract

The enteric nervous system (ENS) is an incredibly complex neural network that is extensively integrated within the neuroimmunoendocrine system through countless signalling pathways that have yet to be fully characterized. In the last decade we have discovered that many more neurotransmitters are at work in the ENS than was originally thought. This opens up new avenues of research into physiological phenomena traditionally thought to be associated only with the central nervous system, such as NMDA receptor-induced excitotoxicity, and how these may influence immune interactions. In particular, the kynurenine pathway catabolism of tryptophan produces many neuro-active and immuno-active constituents whose effects are unknown in the ENS but are of great consequence in many neurodegenerative disorders of the CNS. Our study hypothesized that co-culture of the enteric neurons with mast cells would increase neuronal survival through kynurenic acid production in quinolinic acid (QUIN)-induced excitotoxic conditions.

This study developed a novel *in vitro* co-culture system of enteric neurons and glia grown from murine longitudinal muscle-myenteric plexus tissue and bone marrow-derived mast cells. In addition, a pipeline in image analysis software CellProfiler was designed and optimized in order to reduce human bias and error in subsequent immunocytochemical image analysis. Furthermore, we identified the genetic expression of subunits of the NMDA glutamate receptor in cultured enteric neurons via PCR, which suggests that these cultured neurons may be susceptible to excitotoxicity. PCR analysis of cultured mast cells seemed to indicate that our cultured mast cells express both *Kmo* and *Kat*, the enzymes needed to produce the neurotoxic QUIN and neuroprotective KYNA, respectively. Overall, co-culture with mast cells seemed to decrease neuronal survival. This project developed a novel methodology for the *in vivo* study of mast cell-nerve interactions, and lays the groundwork for future studies in excitotoxicity in the ENS.

Acknowledgements

I would like to thank Dr. Paul Forsythe for his unending support, as well as Dr. John Bienenstock and Dr. Wolfgang Kunze for their incredible knowledge and guidance through this process. I would also like to thank all of the members of the Forsythe, Bienenstock, and Kunze labs for their help in my experiments and for keeping me on track. I would especially like to thank my mentors and friends Tanvi Javkar and Christine West who have been there for me every step of the way since I joined the lab three years ago. Finally, I would like to thank my partner Alex for his unending support and editing, and my two cats for their emotional support.

Table of Contents

Lay Abstract	ii
Abstract	iii
Acknowledgements	iv
Index of Tables and Figures	vii
Chapter 1: Background	11
1.1 Mast Cell-Nerve Interactions	11
1.2 Excitotoxicity	13
1.3 Excitotoxicity in the Enteric Nervous System.....	14
1.4 The Kynurenine Pathway	16
1.5 Irritable Bowel Syndrome	19
Chapter 2: Hypothesis and Project Aims	20
2.1 Hypothesis	20
2.2 Specific Aims	20
Chapter 3: Methodology	21
3.1 Murine LMMP Neuronal Culture.....	21
3.2 Murine Bone Marrow-Derived Mast Cell (BMMC) Culture	22
3.3 Enteric Neuron and BMMC Co-Culture	23
3.4 Immunofluorescence	23
3.5 SK-N-SH Cell Line Culture	25
3.7 PCR.....	26
3.8 DNA Gel.....	26
3.9 Image Analysis	27
Chapter 4: Results	29
4.1 Methods Development.....	29
4.2 Aim 1 Results	30
4.3 Aim 2 Results	32
4.4 Aim 3 Results	33
Chapter 5: Discussion	35
Chapter 6: Conclusions	39
Appendix	40
A.1 BMMC Culture Protocol (Adapted from Khambati et al., 2017).....	40
A.2 LMMP Culture Protocol (Adapted from Smith et al., 2013).....	42

A.3 CellProfiler Pipeline	46
Bibliography	53

Index of Tables and Figures

Figure 1: Mechanisms of mast cell-nerve communication. Mast cells communicate with nerves through integrin signalling and transgranulation while in close contact, and the majority of the time through paracrine signalling (Forsythe, 2019). Used with permission.	12
Figure 2: A cross-section of the mammalian ileum outlining the location of the myenteric plexus.	15
Figure 3: The kynurenine pathway of the tryptophan catabolism. Kynurenic acid (KYNA), highlighted in blue, is a neuroprotective NMDA antagonist, whereas the further downstream metabolites quinolinic acid (QUIN) and 3-hydroxy-L-kynurenine highlighted in red are excitotoxic.	18
Figure 4: Experimental setup. LMMP culture or the SK-N-SH cell line were plated onto glass coverslips pre-coated with poly-L-lysine and natural mouse laminin (Invitrogen) in a 24 well plate. Treatment was then added after cells reached maturity (5 days after seeding for LMMP, 48 hours after plating for SK-N-SH cells).....	22
Figure 5: A sample fluorescence microscopy image taken on day 5 of the LMMP neuronal culture. Cell nuclei are stained in blue with DAPI, and neuronal processes are stained with β -III-tubulin in green.	24
Figure 6: A sample fluorescence microscopy image of SK-N-SH neuroblastoma cells stained with beta-III-tubulin and propidium iodide. This image is a composite image of 16 images taken in a 4x4 grid on the slide.	25
Figure 7: A sample readout of an object-identifying module in CellProfiler.	27
Figure 8: DNA gel showing NMDAR subunit expression (Nr2a,b,c) and kynurenine pathway enzymes (Kat, Kynu) expression in the hippocampus, the LMMP culture, and the BMMC culture. The lack of Nr1 expression in the hippocampus indicates a failure in primer design that was corrected in subsequent tests.	31
Figure 9: DNA gel showing NMDAR subunit expression (Nr1, Nr2a,b,c) and kynurenine pathway enzymes (Kmo, Kat, Kynu) expression in the hippocampus, the LMMP culture, the liver, and the BMMC culture. This figure shows that after a primer redesign, Nr1 was appropriately expressed in the hippocampus.....	32
Figure 10: DNA gel showing kynurenine pathway enzyme expression in the BMMC culture as compared to a spleen positive control.	32

Figure 11: LDH assay results on supernatant from the LMMP myenteric neuron culture (ENC) with and without BMMC co-culture. The bars display standard error of the mean (SEM). 34

Figure 12: Immunocytochemistry results from the SK-N-SH cell culture with 48-hour treatments of QUIN and KYNA. The bars display standard error of the mean (SEM). 34

List of Abbreviations and Symbols

AMPA receptor – α -amino-3-hydroxy-5-methyl-4-isoxazolepropionic receptors
ANS – Autonomic nervous system
BMDC – Bone marrow-derived mast cells
BSA – Bovine serum albumin
BSA-PBS – Bovine serum albumin-phosphate-buffered saline
Ca²⁺ – Calcium ions
CNS – Central nervous system
CO₂ – Carbon dioxide
CRH – Corticotropin-releasing hormone
DAPI – 4',6-diamidino-2-phenylindole
DNA – Deoxyribonucleic acid
EDTA – Ethylenediaminetetraacetic acid
ENC – Enteric neuron culture
ENS – Enteric nervous system
FBS – Fetal Bovine Serum
FcεR1 – Fc epsilon receptor 1 (high-affinity IgE receptor)
GDNF – Glial-derived neurotrophic factor
GI – Gastrointestinal
HBSS – Hank's Buffered Saline Solution
HPLC – High performance liquid chromatography
IBS – Irritable bowel syndrome
IBD – Inflammatory bowel disease
IDO – Indoleamine 2,3-dioxygenase
IgE – Immunoglobulin E
IL-3 – Interleukin-3
KAT – Kynurenine aminotransferase III
KMO – Kynurenine-3-monooxygenase
KYNA – Kynurenic acid
LDH – Lactate dehydrogenase
LMMP – Longitudinal muscle/myenteric plexus
MEM – Minimum essential medium
nAChRs – Nicotinic acetylcholine receptors
NAD⁺ – Nicotinamide adenine dinucleotide
NGF – Neural growth factor
NMDA receptor – N-methyl-D-aspartate receptor
PAR2 – Proteinase-activated receptor₂
PBS – Phosphate-buffered saline
PCR – Polymerase chain reaction
PI – Propidium iodide
QUIN – Quinolinic acid
RNA – Ribonucleic acid
SCF – Stem cell factor
SEM – Standard error of the mean
TAE – Tris-acetate-EDTA

TUNEL assay – Terminal deoxynucleotidyl transferase dUTP nick end labeling
assay
UV – Ultraviolet

Chapter 1: Background

1.1 Mast Cell-Nerve Interactions

Mast cells are often called the sentinels of innate immunity because of the number of diverse functions they serve to protect against invading bacterial and parasitic pathogens, as well as venomous stings and bites (Rivera, 2006). They are granulocytes distributed throughout the body in critical locations where pathogens are likely to be found; namely, on the borders to the external environment, such as mucosal membranes, the blood brain barrier, and near the vasculature. In this capacity, they signal disturbances or immune challenges in the local environment to other immune cells, helping to initiate the innate immune response (Forsythe, 2019; Forsythe & Bienenstock, 2012). There are two main types of mast cell in rodents: mucosal mast cells, and connective tissue mast cells, named after the types of tissue in which they are found. Each of these types express a distinct set of mediators and are distinct in both morphology and physiology. In humans, mast cells have been classified into three subtypes based on their protease content: mast cells that only contain chymase, mast cells that only contain tryptase, and mast cells that contain chymase, tryptase, carboxypeptidase, and cathepsin G (Forsythe, 2019). Mast cells display a great deal of plasticity and are capable of transdifferentiation into other types even after differentiation (Kitamura, 1987).

While they are well known for their role in the allergic response through the IgE-mediated activation of the Fcε receptor 1 (FcεRI), evolutionarily, it is thought that primordial mast cells predate the existence of vertebrates (Wong et al., 2014). This suggests that mast cells serve important beneficial functions besides the ones mediated through IgE, as invertebrates do not possess an immunoglobulin-centred adaptive immune system (Kumar and Sharma, 2010). Additional evidence to suggest this comes from the observation that mast cells are commonly found in

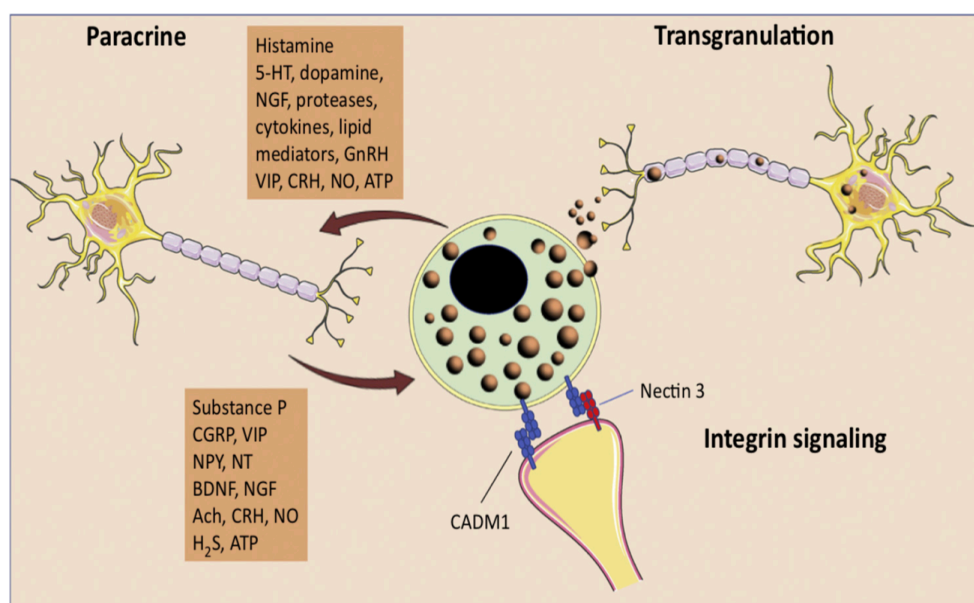


Figure 1: Mechanisms of mast cell-nerve communication. Mast cells communicate with nerves through integrin signalling and transgranulation while in close contact, and the majority of the time through paracrine signalling (Forsythe, 2019). Used with permission.

close proximity to nerves, despite their proficiency at inciting inflammation (Gamble and Goldby, 1961). From an evolutionary perspective, this suggests that there may be an adaptive benefit of putting them so close to nerves. It is easy to conceive that the communication between mast cells and nerves may have been important enough to warrant this risk, although there is still currently a lack of understanding of these proposed neuroimmune connections.

One of the earliest discoveries of neuroimmune communication was the relationship between mast cells and peripheral nerves (Gamble & Goldby, 1961; Newson, Dahlström, Enerbäck, & Ahlman, 1983). In the mammalian nervous system, neurons and mast cells are located in very close proximity to one another, with some neurites even extending into direct contact with mast cells. These physical synapses between mast cells and nerves are able to modulate the functionality of the cell, as well as its phenotype through integrin signalling (Hagiya et al., 2011; Suzuki, Suzuki, Furuno, Teshima, & Nakanishi, 2004). When nerves are in close proximity to them, mast cells can communicate via the transfer of their granule contents in a process called transgranulation (Wilhelm,

Silver, & Silverman, 2005). Through this process, which is hypothesized to involve modulating intracellular Ca^{2+} , mast cells can modify their microenvironment, and even the function of the neurons around them. This suggests that they could play a neuroprotective role through the release of these mediators (Jonas, Sugimori, & Llinás, 1997). Mast cells also use paracrine signalling to communicate with nerves. They also synthesize and secrete many neuroactive mediators, such as monoamines like serotonin and dopamine, nerve growth factor (NGF), and neuropeptides such as corticotropin releasing hormone (CRH) (Leon et al., 1994). These three major signalling pathways between nerves and mast cells are outlined in Figure 1. Although mast cells communicate with nerves in this way in the central nervous system (CNS) as well as the periphery, the focus of this dissertation is on their signalling in the periphery, and more specifically in the enteric nervous system, where they are present in much higher numbers. (Edvinsson et al., 1977; Bauer and Razin, 2000).

1.2 Excitotoxicity

Excitotoxicity occurs when excessive stimulation of excitatory glutamate receptors, such as N-methyl-D-aspartate (NMDA) receptors and α -amino-3-hydroxy-5-methyl-4-isoxazolepropionic (AMPA) receptors, causes high levels of calcium ions (Ca^{2+}) to enter the cell. The concentration of free-floating Ca^{2+} in the mammalian cytoplasm is very low – ranging from 10 nM - 100 nM in normal physiological conditions. This is estimated to be 10,000 - 100,000 times the concentration of extracellular Ca^{2+} , which allows for Ca^{2+} to activate many intracellular enzymes and second messenger pathways (Clapham, 2007). As such, intracellular Ca^{2+} is under the tight control via various buffering, storage, and binding mechanisms inside the cytoplasm. In excitotoxic conditions, this rapid and sustained influx of large amounts of Ca^{2+} overruns the cell's Ca^{2+} buffering mechanisms and allows Ca^{2+} to activate many enzymes including proteases, phospholipases, and calpain, which then damage the cell and lead to apoptosis

(Jaiswal et al., 2009; Manev, Favaron, Guidotti, & Costa, 1989). Excitotoxicity has been implicated in many neurodegenerative diseases affecting the CNS, including Alzheimer's disease (Molinuevo, Lladó, & Rami, 2005), multiple sclerosis (Pitt, Werner, & Raine, 2000), amyotrophic lateral sclerosis (ALS) (Leigh & Meldrum, 1987) Parkinson's disease (M. Flint Beal, 1998), Huntington's disease (Tabrizi et al., 1999), depression and suicide (Bryleva & Brundin, 2017), alcohol and benzodiazepine addiction and withdrawal (Hughes, 2009), spinal cord injury (Azbill, Mu, Bruce-Keller, Mattson, & Springer, 1997) stroke (Choi, 2017), and traumatic brain injury (Werner & Engelhard, 2007).

1.3 Excitotoxicity in the Enteric Nervous System

The enteric nervous system (ENS) is a division of the autonomic nervous system (ANS) that is embedded in the lining of the gastrointestinal (GI) tract and governs its motor functioning, local blood flow, mucosal transport, and secretions. It is often called the “second brain” due to its ability to function independently and its complexity. The ENS is comprised of two main ganglia: the myenteric plexus, which is located between the longitudinal and circular muscle layers, and the submucosal plexus, which is located in the submucosa (Figure 2) (Furness, 2006).

The function of rapid excitatory neurotransmission in the ENS is mostly fulfilled by cholinergic neurotransmission through nicotinic acetylcholine receptors (nAChRs), although over 30 other types of neurotransmission occur, the most abundant of which being serotonergic and the more recently discovered dopaminergic signalling (Li, Pham, Tamir, Chen, & Gershon, 2004; Martinucci et al., 2015). With such a multitude of neuronal signalling, it seems unlikely that glutamate, the most abundant neurotransmitter in vertebrates, would not be involved. Multiple lines of evidence suggest that glutamate acts as an excitatory neurotransmitter in the gut (Bian, Zhou, & Galligan, 2004; Galligan, LePard, Schneider, & Zhou, 2000; Liu, Rothstein, Gershon, & Kirchgessner, 1997; Wiley, Lu, & Owyang, 1991) Several of these studies found excitatory glutamatergic neurons in the ENS in rodents (Burns and Stephens, 1995). Indeed, there are reports of gut reflexes that occur independently of cholinergic excitatory

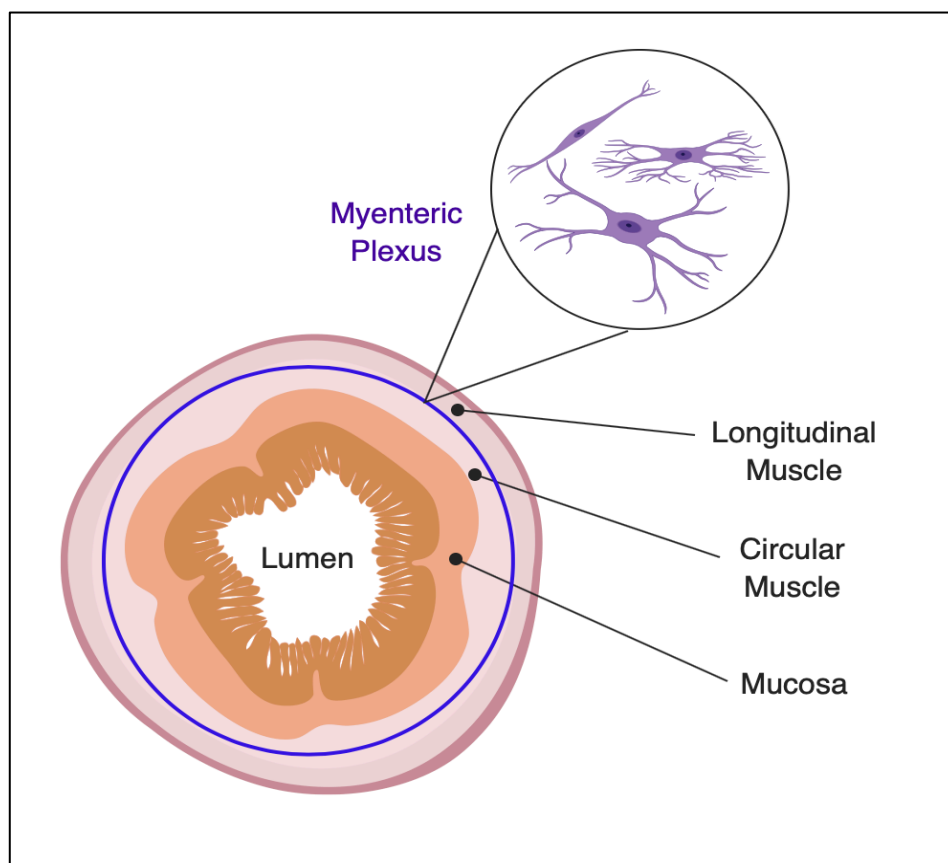


Figure 2: A cross-section of the mammalian ileum outlining the location of the myenteric plexus.

transmission (Galligan et al., 2000). Ionotropic glutamate receptors have been found to play a role in visceral nociception in rats, and metabotropic glutamate receptors have been characterized in the submucosal plexus of the guinea pig ileum (Hu et al., 1999; Reis et al., 2000).

However, the fact as to whether or not glutamate has a similar excitatory functionality in the enteric nervous system remains inconclusive, as evidenced by differing opinions on the access that intravascular macromolecules from dietary glutamate would have to the ENS (Gershon & Bursztajn, 1978; Wang, Wang, Xia, & Wood, 2014). Some studies have found glutamate-induced excitotoxicity to be present in the ENS, (Kirchgessner, Liu, & Alcantara, 1997), however the findings have yet to be repeated. If excitotoxicity were taking place in the ENS, it would thus foreseeably play an important role in the crosstalk within the neuroimmunoendocrine system and the gut microbiome, since many immune cells are capable of making and excreting excitotoxic compounds. One of these more notable compounds is quinolinic acid (QUIN), an NMDA receptor agonist, which is produced by activated microglia (Guillemin, Smythe, Takikawa, & Brew, 2005). QUIN is one of the many neuroactive metabolites produced via the catabolism of tryptophan through kynurenine pathway, which many types of immune cells, nerves, and bacteria are capable of performing (Kennedy, Cryan, Dinan, & Clarke, 2017; O'Mahony, Clarke, Borre, Dinan, & Cryan, 2015).

1.4 The Kynurenine Pathway

The kynurenine pathway is the major metabolic pathway in the metabolism of the essential amino acid tryptophan. This pathway forms many neuroactive intermediates and ultimately leads to the production of nicotinamide adenine dinucleotide (NAD⁺), a metabolic cofactor found in all living cells. Some of these metabolites have been widely implicated in many aforementioned diseases in which excitotoxicity occurs, including kynurenic acid (KYNA), QUIN (Boegman,

El-Defrawy, Jhamandas, Beninger, & Ludwin, 1985; Braidy, Grant, Adams, Brew, & Guillemin, 2009), and more recently, 3-hydroxyanthrallic acid and anthranillic acid (Darlington et al., 2010). Quinolinic acid has been most extensively studied and is known to be a relatively selective NMDA receptor agonist that induces neurotoxic and gliotoxic effects via oxidative stress and excitotoxicity (Cruz, Carrillo-Mora, & Santamaría, 2013; Guillemin, 2012; Lugo-Huitrón et al., 2013). Its toxicity arises from NR2A and NR2B NMDA receptor activation leading to excitotoxicity, lipid peroxidation, and increased glutamate concentrations in the extracellular environment (Guillemin, 2012) While any immune mediators such as astrocytes, neurons, and mast cells can catabolize QUIN (Guillemin et al., 2005), only microglia and infiltrating macrophages can produce it in the central nervous system (CNS), with macrophages having approximately 30 times the productive capacity as compared to microglia (Espey, Chernyshev, Reinhard, Namboodiri, & Colton, 1997; Guillemin, 2012; Guillemin

et al., 2005). In contrast, KYNA has been shown to be a neuroprotective NMDA antagonist, countering the neurotoxic effects of QUIN (Boegman et al., 1985). These metabolites are formed through two separate processes competing for kynurenine as a substrate, often referred to as the neurotoxic and neuroprotective “arms” of the kynurenine pathway, as shown in Figure 3 (Oxenkrug, 2010). IDO, the rate-limiting enzyme of the kynurenine pathway, is also of particular interest because it is induced by interferon γ , and in turn activates T regulatory cells and suppresses T cells and NK cells, promoting immune tolerance (Taylor and Feng,

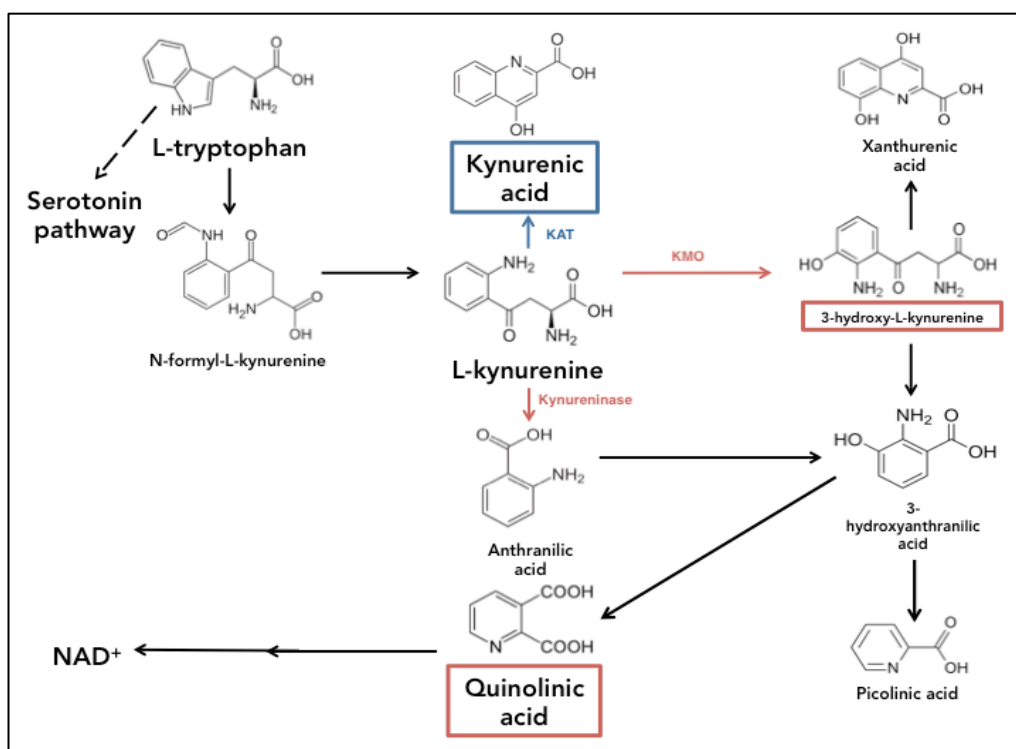


Figure 3: The kynurenine pathway of the tryptophan catabolism. Kynurenic acid (KYNA), highlighted in blue, is a neuroprotective NMDA antagonist, whereas the further downstream metabolites quinolinic acid (QUIN) and 3-hydroxy-L-kynurenine highlighted in red are excitotoxic.

1991; Campbell, Charych, Lee and Möller, 2014). Thus, this pathway is closely intertwined with the functioning of both the nervous system and the immune system, making it a crucial area of research for many inflammatory diseases.

1.5 Irritable Bowel Syndrome

Irritable Bowel Syndrome (IBS) is a very common illness, which affects an estimated 10-15% of people in North America, and accounts for 25-50% of all referrals to all gastroenterologists (Saito, Schoenfeld and Locke, 2002). It is characterized by symptoms of visceral pain, disturbed defecation, bloating, and distension without structural or biochemical abnormalities, and its aetiology is poorly understood (Paré et al., 2006). IBS is 2-3 times more common in females than in males, and is a very heterogenic illness, both in its presentation and its pathogenesis (Saito, Schoenfeld and Locke, 2002). Because its presentation is so varied, IBS is sub-categorized into three main groups: IBS-predominantly constipation (IBS-C), IBS-predominantly diarrhoea (IBS-D), and IBS-mixed (IBS-M). There is also considerable diversity in the pathogenesis of IBS, with some cases emerging exclusively from acute gastroenteritis termed post-infectious IBS, and some seemingly deriving only from environmental, psychosocial, and genetic factors (Chey, Kurlander and Eswaran, 2015).

Certain subsections of IBS patients have been shown to have an increased presence of proinflammatory immune cells in the intestinal mucosa, which may play a role in the heightened visceral hypersensitivity and disturbed sensory-motor functions seen in IBS (Barbara et al., 2004). Mast cells are often implicated in this disturbance, because of their close association with nerves and release of proinflammatory and excitatory mediators such as tryptase and histamine (Reed et al., 2003). Despite this pathological role, there is likely a physiological role for mast cell-nerve interactions. One of the most important goals of this project was to understand how mast cell-nerve communication would influence kynurenine pathway-induced excitotoxicity in the ENS, to determine whether mast cells could potentially be neuroprotective in a homeostatic, resting state.

Chapter 2: Hypothesis and Project Aims

2.1 Hypothesis

In physiologically relevant numbers, resting bone marrow-derived mast cells (BMMCs) will protect neurons from QUIN-induced excitotoxicity in a murine *ex vivo* longitudinal muscle myenteric plexus (LMMP) tissue culture model of enteric neurons and glia.

2.2 Specific Aims

1. To determine if neurons cultured from murine LMMP have NMDA receptors
2. To determine if BMMCs are capable of producing metabolites from only the neuroprotective arm of the kynurenine pathway:
 - a) To determine if BMMCs are capable of producing quinolinic acid (QUIN)
 - b) To determine if BMMCs are capable of producing kynurenic acid (KYNA)
3. To determine if co-culturing murine myenteric neurons with BMMCs decreases cell death in excitotoxic conditions

Chapter 3: Methodology

3.1 Murine LMMP Neuronal Culture

We used the method of culturing murine enteric neurons from the LMMP of the jejunum and ileum of adult Swiss Webster male mice (Charles River Laboratories) outlined by Smith et al. in 2013. In brief, two adult Swiss Webster mice were culled by cervical dislocation, then their small intestine was harvested up to 10 cm from the caecum and placed in ice-cold 1 M Krebs solution which was bubbled with carbogen for 30 minutes prior to the sacrifice to normalize pH. Next, the intestines were snipped into 2 cm long pieces and flushed with ice-cold Krebs. After flushing and cannulating the intestine on a thin paintbrush, LMMP was carefully stripped from the intestinal wall. After this the tissue was washed, digested in collagenase type II and trypsin, and filtered through Nitrex mesh into complete enteric neuron media (Neurobasal A media (Gibco) with 2% B-27 supplement (Thermo-Fisher Scientific), 0.25% recombinant murine GDNF, 1% 100x Antibiotic-Antimycotic (Gibco), 1% fetal bovine serum, and 1% 200 mM L-glutamine (Gibco)). Then, after mixing for 30 minutes in a rotating mixer, the suspended cell solution was plated onto glass coverslips pre-coated with poly-L-lysine and natural mouse laminin (Invitrogen) in a 24 well plate (Figure 4). This procedure yields electrophysiologically functional enteric neurons and glia on the third day after plating, and neurons can survive up to seven days after plating (Smith, Ngwainmbi, Grider, Dewey, & Akbarali, 2013). After 5 days, the cells were used for experiments. Sample fluorescence microscopy images are shown in Figures 5 and 6.

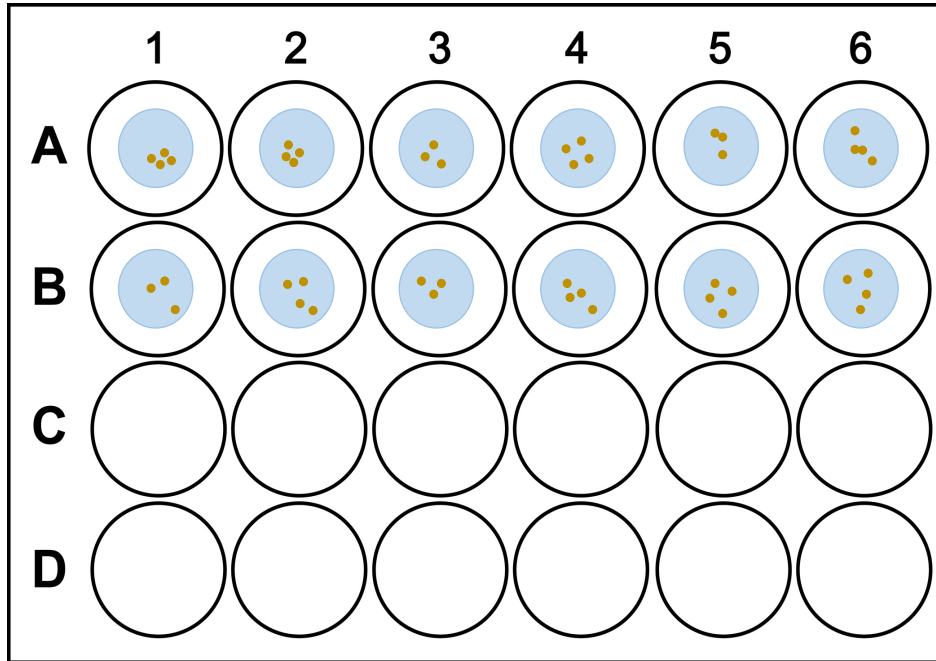


Figure 4: Experimental setup. LMMP culture or the SK-N-SH cell line were plated onto glass coverslips pre-coated with poly-L-lysine and natural mouse laminin (Invitrogen) in a 24 well plate. Treatment was then added after cells reached maturity (5 days after seeding for LMMP, 48 hours after plating for SK-N-SH cells).

3.2 Murine Bone Marrow-Derived Mast Cell (BMMC) Culture

The method of culturing murine mast cells was acquired from (Khambati, Han, Pijnenburg, Jang, & Forsythe, 2017). In brief, two 6-8 week old male Balb/c mice (Charles River Labs) were culled via cervical dislocation and their femurs were harvested and stored on ice in BMMC medium (RPMI medium (Gibco), with 10% fetal bovine serum (Gibco) by volume, 1% penicillin/streptomycin (Gibco) by volume, 200 μ L of 1 mM SCF and 1 mM IL-3 solution (in ddH₂O, stored at -20 °C), and supplemented with 30 mL of a pre-made supplement solution of 29 μ L of β -mercaptoethanol (Gibco), 3 mL of 200 mM L-glutamine (Gibco), and 5 mL 20x MEM (Gibco) topped to 500 mL with deionized water. The bone marrow was harvested from the femurs in sterile conditions by snipping the ends of each femur and then flushing the bones with medium into a falcon tube. Next, the bone marrow was spun down, resuspended in 10 mL of BMMC medium, counted, and seeded at a concentration of 2.0×10^5 cells/mL in 20 mL media in T-75 flasks

(Sarstadt). Flasks were changed every week with fresh 20 mL BMMC medium, and after four weeks the culture were virtually fully differentiated into mast cells.

3.3 Enteric Neuron and BMMC Co-Culture

On the fifth day after plating the myenteric neurons, they were treated with QUIN, KYNA, L-kynurenine, (Sigma-Aldrich), Ca^{2+} ionophore A23187 (Sigma-Aldrich), or vehicle with or without BMMCs. Concentrations of kynurenine pathway metabolites were based on the paper that first showed that KYNA inhibits the excitotoxic action of QUIN in hippocampal neurons (Boegman et al., 1985). The concentrations were then modified through trial and error, in order to find a suitable concentration. BMMCs were added in physiologically relevant concentrations of approximately 10 LMMP cells to 1 BMMC. Ratios were calculated based on an estimation of an average of 10,000 cells per LMMP culture coverslip. This estimation was approximated by averaging total cell numbers per slide with fluorescence microscopy. The investigators acknowledge that this is not a very robust method; however, methods to count the cells on the coverslips without staining them were extremely limited. BMMCs were added in their own media, but in a very small volume (10 μL) to avoid effects based on the change of media. They were then placed in an incubator at 37°C and 5% CO_2 for 24 hours before aspirating out the medium and fixing the cells on the coverslips with ice-cold 100% methanol for 10 minutes. They were then stored in sterile 1% BSA-PBS in a 4°C refrigerator for up to a week until immunofluorescence.

3.4 Immunofluorescence

Coverslips were rinsed 3 times with PBS and then incubated in 1:500 anti-mouse β -III-tubulin (abcam ab18207) in sterile 1% BSA-PBS overnight in the dark at 4°C. The next day, the coverslips were again rinsed 3 times with PBS before adding 1:1000 AlexaFluor 488 (Thermo-Fisher Scientific) as a secondary

antibody. After a 1-hour incubation in the dark, the secondary antibody was aspirated and each of the slips was washed 3 times with PBS. Next, 1 mg/mL propidium iodide (PI) solution (Thermo-Fisher Scientific) was added to each of the wells containing the coverslips and they were left to sit at room temperature in

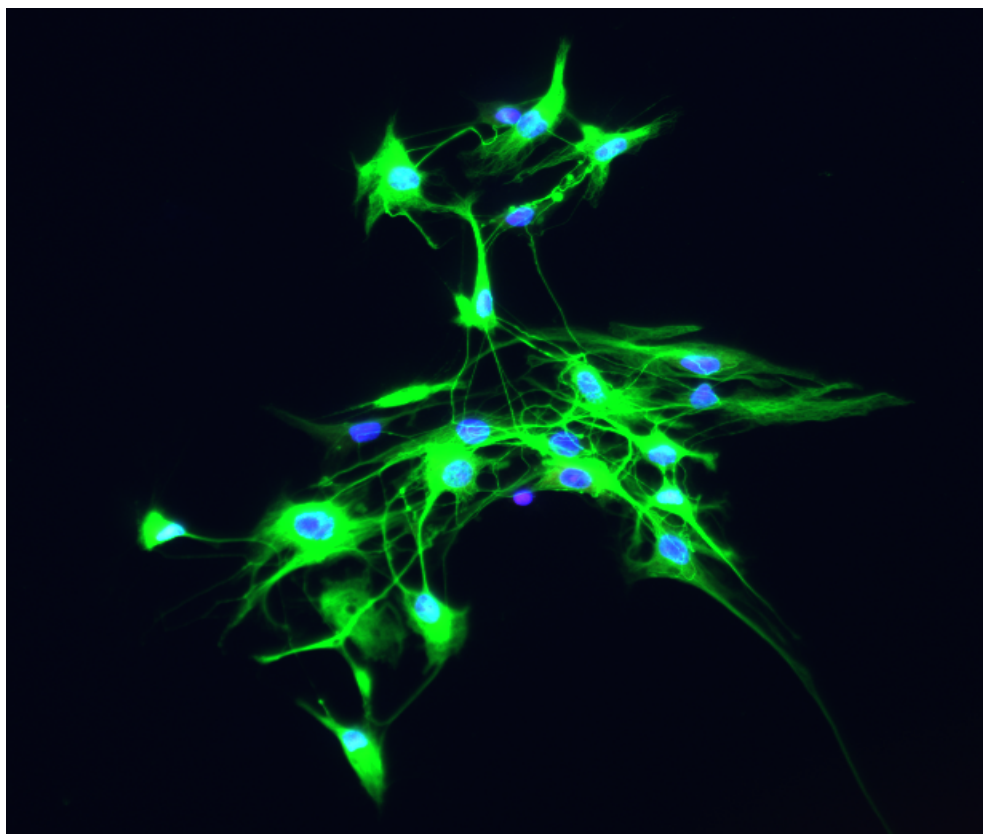


Figure 5: A sample fluorescence microscopy image taken on day 5 of the LMMP neuronal culture. Cell nuclei are stained in blue with DAPI, and neuronal processes are stained with β -III-tubulin in green.

the dark for 5 minutes. The PI was aspirated, and the coverslips were rinsed 3 times with PBS before mounting onto slides with ProDiamond Anti-Fade Mounting Medium (Thermo-Fisher Scientific), or in the initial trials when PI was not used, with ProDiamond Anti-Fade Mounting Medium with DAPI (Thermo-Fisher Scientific). After sitting in the mounting medium in the dark for 30 minutes, coverslips were sealed onto the slides with clear nail polish and imaged using a Zeiss Imager Z.1 Series fluorescence microscope in a dark room.

3.5 SK-N-SH Cell Line Culture

The SK-N-SH cell line is the only cell line that expresses a fully functional NMDA receptor, and so it was used as a positive control. The SK-N-SH cell line was obtained from ATCC and cultured according to their specifications. Culture medium was made by adding 10% fetal bovine serum by volume, 1% 100x minimum essential medium-non-essential amino acids (MEM-NEAA) (Gibco) by volume, 1% 100 μ M sodium pyruvate by volume (Gibco), and 1% Pen-Strep (Gibco) by volume to 500 mL of minimum essential media (MEM) (Gibco). The cells were seeded into T-25 cell culture flasks (Sarstadt) at a concentration of

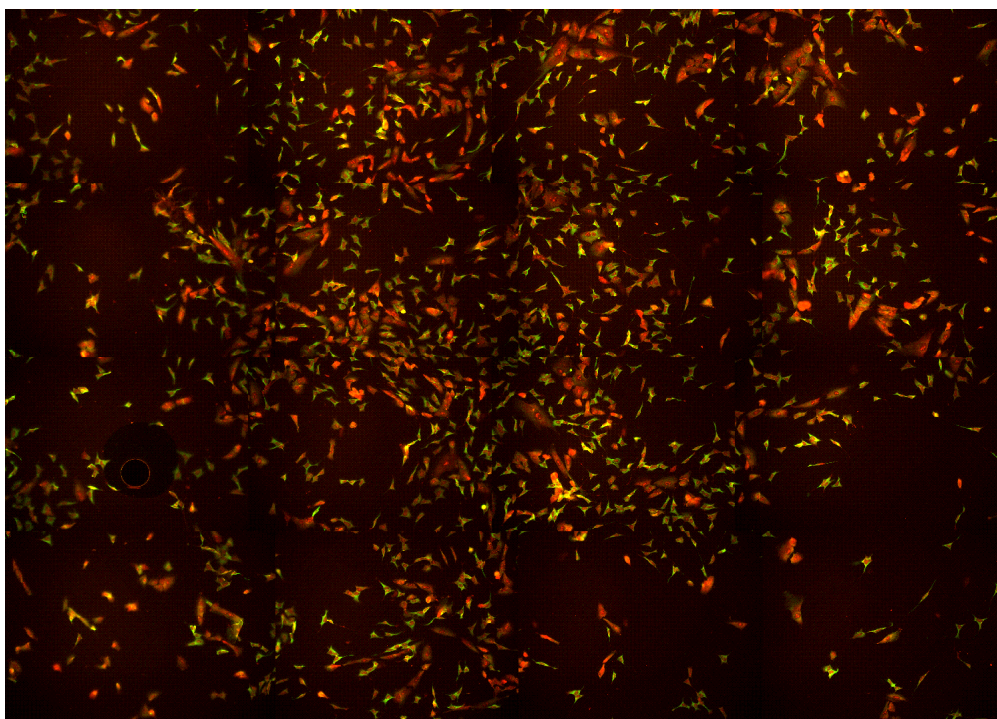


Figure 6: A sample fluorescence microscopy image of SK-N-SH neuroblastoma cells stained with beta-III-tubulin and propidium iodide. This image is a composite image of 16 images taken in a 4x4 grid on the slide.

approximately 1 million cells/mL and when confluent, were passaged using 0.25% Trypsin (Gibco) and seeded into larger T75 flasks (Sarstadt). Following this, the media was changed every 3 days, and the cells were passaged every

week. The cells were seeded onto glass coverslips pre-coated with poly-L-lysine and natural mouse laminin (Invitrogen) in a 24 well plate (Figure 4).

3.6 Primer Design

Primers were originally selected from published literature on PubMed, however these primers did not work in the cycling conditions used in this study. Therefore, Primers were designed using data from UniProt and BLAST (U.S. National Institutes of Health, 2019). After the protein of interest was found on UniProt, the FASTA sequence was copied and searched in tBLASTn to search for translated nucleotides for the proteins. Finally, the nucleotides were used to find primers using primerBLAST. Primers were selected based on their validation by other investigators and their melting temperature.

3.7 PCR

QuantDesign Studio software was used to design plate diagrams and temperature cycling. RNA was extracted from 1 million cells using the Qiagen RNeasy kit according to the manufacturer's instructions. In the case of the LMMP culture, cells were scraped off of the glass coverslips using mini cell scrapers (Invitrogen). For brain tissue, the RNeasy Lipid Tissue Kit was used according to the manufacturer's instructions. Eluted RNA was stored at -80°C in the dark until cDNA transcription. cDNA was transcribed using SuperScript IV VILO Master Mix with ezDNase Enzyme (Invitrogen) according to the manufacturer's instructions, and then stored in at -80°C in the dark until PCR was run.

3.8 DNA Gel

Agarose gel was prepared by mixing 100 mL 1x TAE Buffer (ThermoFisher Scientific) with 2 g Ultrapure Agarose (ThermoFisher Scientific) in a 250 mL

Erlenmeyer flask and then heating it on high in the microwave for 30 seconds at a time, in between runs, until a clear gel was formed. This gel was then mixed with 1 μ L SYBR Safe dye (Invitrogen) until evenly distributed and then poured slowly into a large gel tray and left for 45 minutes until the gel was set. The comb was removed from the tray and the gel was submerged in the running tank in 1x TAE buffer. 10 μ L of PCR sample was mixed with 2 μ L DNA Gel Loading Dye (6x) (Thermo Scientific) and added to the lanes along with a 100 bp DNA Ladder (Invitrogen). The separation was completed in approximately 90 minutes at 50 V, and the gel was visualized on an UV transilluminator.

3.9 Image Analysis

The free open source image analysis software CellProfiler was used to analyze the fluorescent microscopy images (Carpenter et al., 2006). This software was used to classify and count neurons based on their β -III-tubulin fluorescence intensity

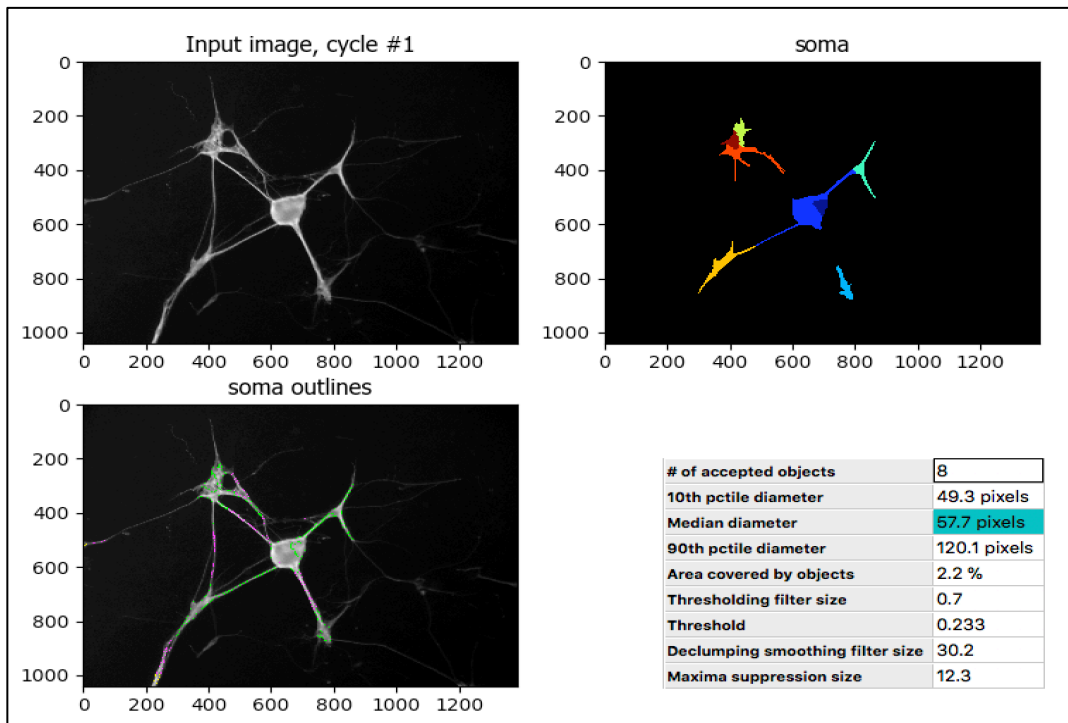


Figure 7: A sample readout of an object-identifying module in CellProfiler.

values, their propidium iodide (PI) fluorescence intensity values, as well as their size, and shape (see Figure 7). The created algorithm is composed of a list of modules in a particular order, that each performs a specific function and the complete algorithm was called a “pipeline”. The created pipeline used filtering modules to exclude objects in images with average intensity values under a specified threshold. The thresholds were chosen by comparing counts completed by the program and manual counts completed by the investigator. After objects were filtered according to their intensity of β -III-tubulin fluorescence and their intensity of PI fluorescence, they were further filtered by minimizing the distance from the centroid of an object stained for β -III-tubulin and any objects in close proximity stained for PI, in order to make sure that only objects that were both β -III-tubulin positive (neuronal) and PI positive (dead) were counted. The β -III-tubulin positive cells that met the condition of being above the intensity threshold and having a proximal cell that was above the intensity threshold for PI were counted as dead neuronal cells. The full pipeline is shown in the Appendix.

Chapter 4: Results

4.1 Methods Development

The nature of this project was very exploratory, and since there was little previous work – both from our lab and within the literature – done on this kind of *in vitro* system, much of the methodology was developed over the course of the thesis.

The program CellProfiler was chosen for this study in order to create a consistent, replicable, and precise method of classifying and counting cells from hundreds of fluorescence microscopy images. This method was also chosen in order to minimize the potential for investigator bias in manual counting. CellProfiler has many built-in “modules”, which are small programs that perform various tasks on the uploaded images, such as classifying cells according to size or shape, or measuring the average intensity of objects in the images. Each of these modules were configured and optimized individually so that they would be able to perform their task appropriately according to the types of images they were given. Once all of the modules are added, the program runs them in the order instructed and produces outputs accordingly, and then consolidates all of this data into an exportable spreadsheet.

Because the modules rely on cell size, shape, and fluorescence intensity for classification, the pipeline parameters were slightly modified for each batch of slides. For example, in order to identify which objects to count, the program asks the investigator for a diameter range of an average object. In order to ensure that these modifications were consistent, the range of diameters inputted for each data set was calculated based on the average diameter of the objects and the standard deviation. After careful consideration and several trial runs with each method of edge detection that the program had to offer, Otsu thresholding was determined to be the most accurate method.

Otsu thresholding is a method of identifying the edges of objects in a grayscale image that uses an iterative algorithm to find the threshold that minimizes the foreground and background variance. The algorithm essentially takes a histogram of all of the pixels in the image and sorts them by intensity. It then picks a threshold and divides the histogram into two classes: the foreground and the background. After going through all of the possible iterations, the algorithm picks the threshold that minimizes the total weighted variance of the foreground and background classes, which is called the “within class variance” (Otsu, 1979). This method was the most efficient for the type of images that were analyzed in this project because of the large intensity differences between the fluorescent objects of interest and the darker background.

4.2 Aim 1 Results

It was fundamental to our research question to ascertain whether or not the murine LMMP-derived enteric neuron/glia culture expressed NMDA receptors so that we could probe their response to excitotoxic conditions.

As shown by the DNA gel in Figure 8, the LMMP myenteric neuron culture seems to express all three subunits of the *Nr2* receptor, as the bands are virtually identical to the hippocampus positive control. However, *Nr1* expression is not seen, which is likely due to a failure in *Nr1* primer design, as would be evidenced by the fact that *Nr1*, which according to UniProt is expressed ubiquitously in the brain, is not seen in the hippocampus (National Institutes of Health, 2019). No band is seen for *Kmo*, which, again, is likely due to an issue in primer design, which was remedied in the subsequent trial (Figure 9) Furthermore, expression of kynurenine aminotransferase III (*Kat*) seems consistent across all of the samples, and kynureninase (*Kynu*) seems weakly expressed in all of the samples.

After a redesign of the *Kat* and *Kmo* primers, expression of kynurenine aminotransferase III (*Kat*) and kynurenine-3-monooxygenase (*Kmo*) seem to be expressed in the BMMC culture (Figures 9 and 10), with liver and spleen tissue serving as a positive control for expression.

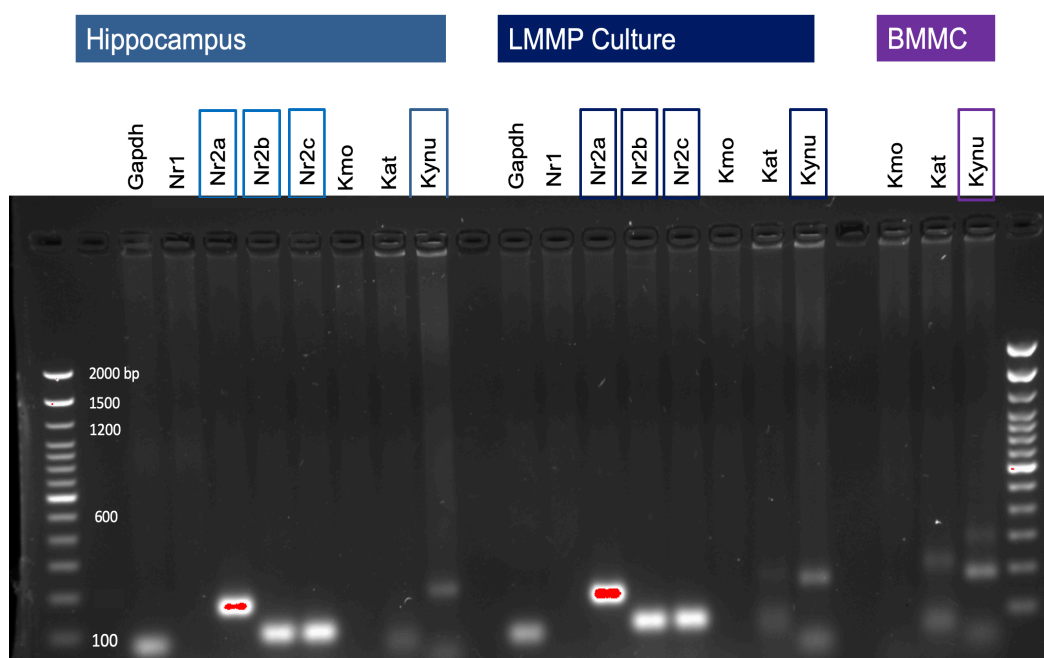


Figure 8: DNA gel showing NMDAR subunit expression (*Nr2a*, *b,c*) and kynurenine pathway enzymes (*Kat*, *Kynu*) expression in the hippocampus, the LMMP culture, and the BMMC culture. The lack of *Nr1* expression in the hippocampus indicates a failure in primer design that was corrected in subsequent tests.

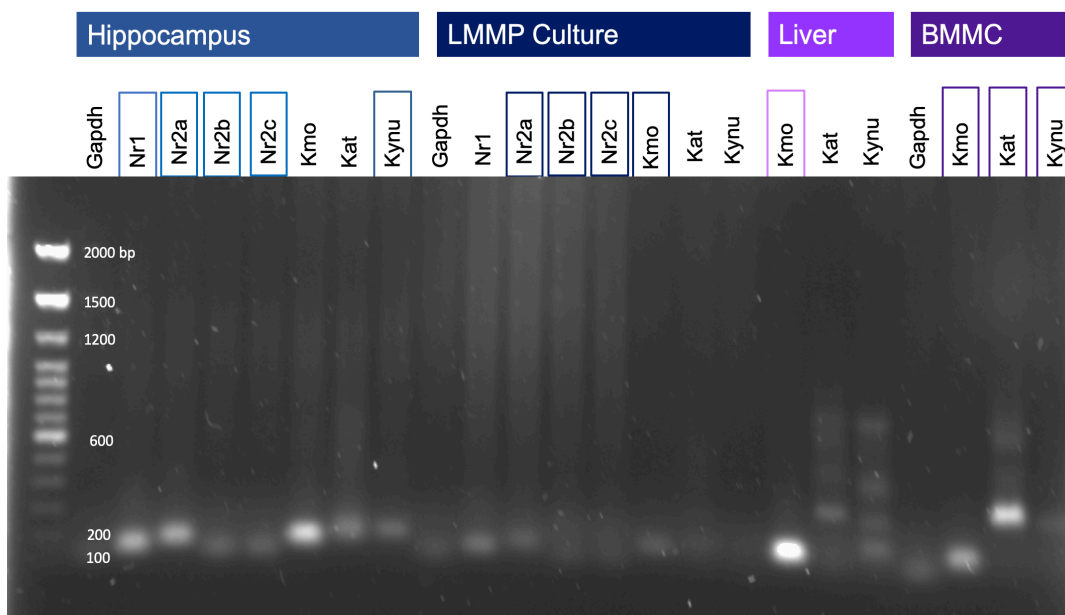


Figure 9: DNA gel showing NMDAR subunit expression (*Nr1*, *Nr2a,b,c*) and kynurenine pathway enzymes (*Kmo*, *Kat*, *Kynu*) expression in the hippocampus, the LMMP culture, the liver, and the BMMC culture. This figure shows that after a primer redesign, *Nr1* was appropriately expressed in the hippocampus.

The SK-N-SH cell line is the only cell line that expresses a fully functional NMDA receptor (Pizzi et al., 2002) and so it was used as a positive control. As shown in Figure 12, there is a trend that shows that the excitotoxin QUIN did seem to dose-dependently kill the neurons, however, there was no rescue of this effect by KYNA.

4.3 Aim 2 Results

As shown in Figures 10 and 11, there seems to be expression of both *Kynu* and *Kat* in the BMMC culture. The liver was chosen as a positive control for the expression of kynurenine pathway enzymes because according to UniProt it is known to have the highest expression of these enzymes

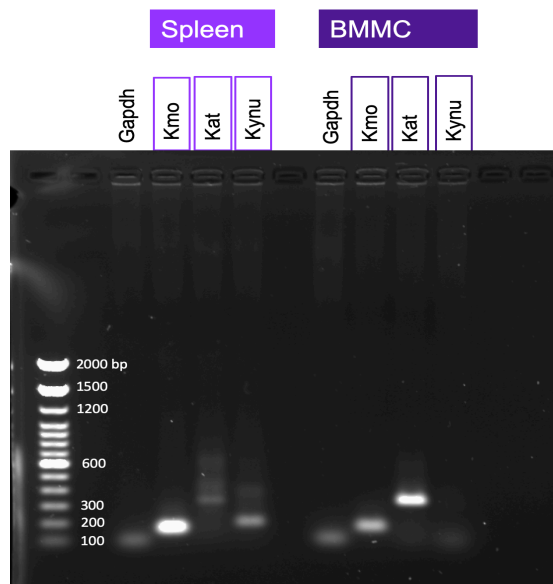


Figure 10: DNA gel showing kynurenine pathway enzyme expression in the BMMC culture as compared to a spleen positive control.

(National Institutes of Health, 2019). However, the range of product sizes suggests that the primers may not be specific enough to be used in the liver, or that primer-dimer formation is occurring, and so the experiment will have to be adjusted to avoid this in future trials. Possible courses of action to avoid non-specific product formation could consist of redesigning the primers or adjusting the cycling conditions during PCR.

4.4 Aim 3 Results

The LDH assay data suggest that, contrary to our hypothesis, the BMNCs may be increasing cell death in co-culture with the myenteric neurons, however, as shown in Figure 11, this is only a trend, that does not reach statistical significance when the groups are compared by ANOVA. Furthermore, this experiment is confounded by inaccurate ratios of BMNCs to LMMP-cultured neurons/glia because of the difficulty of performing an accurate cell count on the neurons/glia before staining, due to their adherence to glass coverslips. This experiment will have to be repeated with a more robust positive control for cell death and a more accurate method of quantifying cell ratios in order to draw any firm conclusions. Further tests with LMMP-derived neurons incubated with BMNCs in QUIN-induced excitotoxic conditions were planned, but were unable to be completed due to time constraints brought on partly by the long maturation period of BMNC cultures (4 weeks) and their extreme sensitivity of both the BMNC and LMMP cultures to changes in their environment (e.g. fluctuations in incubator temperature/humidity, incubator contamination, media pH).

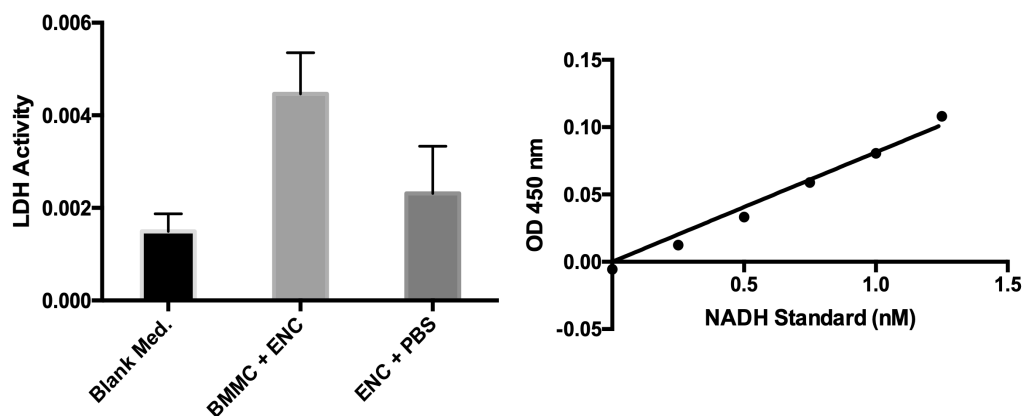


Figure 11: LDH assay results on supernatant from the LMMP myenteric neuron culture (ENC) with and without BMMC co-culture. The bars display standard error of the mean (SEM).

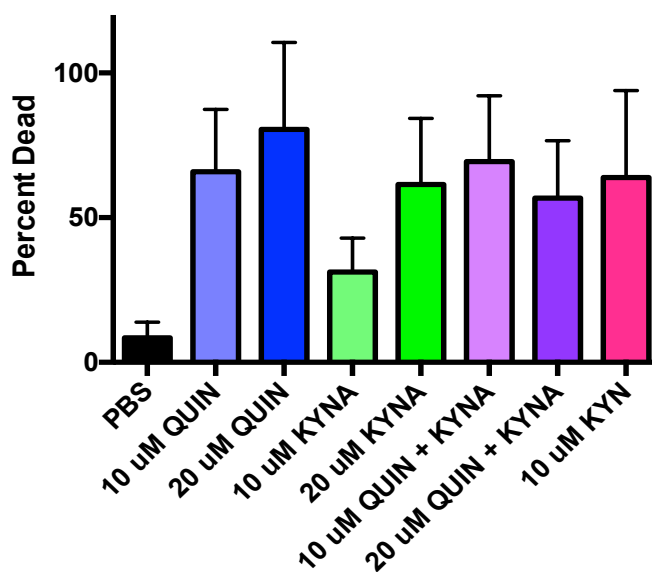


Figure 12: Immunocytochemistry results from the SK-N-SH cell culture with 48-hour treatments of QUIN and KYNA. The bars display standard error of the mean (SEM).

Chapter 5: Discussion

The aim of this study was to understand how mast cell-nerve interactions would influence kynurenine pathway-induced excitotoxicity in the ENS, in order to determine whether mast cells could potentially be neuroprotective in a homeostatic, resting state. In order to further this goal, a custom pipeline made in CellProfiler was designed, tested, and validated in order to analyze immunofluorescence data. This study demonstrated that enteric neurons cultured from murine LMMP express functional glutamate receptors. A new method of co-culturing LMMP-derived myenteric neurons/glia and BMNCs was derived from their existing primary culture protocols. The evidence presented here contradicts our hypothesis that resting mast cells might provide neuroprotection for enteric neurons in an excitotoxic environment.

Relatively little is known about the extent of mast cells' capability to catabolize tryptophan through the kynurenine pathway. Seeing as how other immune cells such as astrocytes and microglia have been shown to favour production of different neuroactive metabolites in this pathway (Guillemin, Smythe, Takikawa and Brew, 2005) (Lim et al., 2017), we postulated that mast cells may have a bias towards producing KYNA, a neuroprotective NMDA receptor antagonist over QUIN, one of the excitotoxic products of the kynurenine pathway. Since mast cells and neurons are physiologically found in close proximity, and partake in bidirectional communication through many different means (Forsythe and Bienenstock, 2012), this neuroprotective capability could help to solve the mystery of the adaptive benefit of coupling nerves and mast cells together. We explored these mast cell-nerve interactions in the context of the kynurenine pathway of the tryptophan catabolism, which has been shown to be implicated in many excitotoxic and inflammatory processes in both neuronal and immune cells (Clarke et al., 2009).

An accumulating body of evidence points toward IBS being regarded as a disorder of the gut-brain axis, with the serotonergic system being a particular point of interest (O'Mahony et al., 2015; Clarke et al., 2009). Serotonin is involved in the regulation of mood, cognition, sleep, and appetite in the CNS (Kim and Camilleri, 2000; Lopez-Ibor, 1992) but the vast majority of serotonin is actually found in the gut, where it regulates the activity of the enteric nervous system and is also used by platelets downstream in the clotting cascade (Berger, Gray and Roth, 2009; Yano et al., 2015). Serotonin is produced by the catabolism of tryptophan through the methoxyindole pathway; although this pathway has generated more research interest, in mammals over 95% of the bioavailable tryptophan is catabolized through the kynurenine pathway. Similar to the methoxyindole pathway, the kynurenine pathway also produces many neuroactive metabolites, such as the NMDA receptor agonist QUIN and the only endogenous NMDA receptor antagonist, KYNA (O'Mahony et al., 2015; Clarke et al., 2009). Further, indoleamine-2,3-dioxygenase (IDO), the rate-limiting enzyme of the kynurenine pathway, is also of particular interest because it is induced by interferon γ and also has immunomodulatory effects (Campbell et al., 2014; Taylor and Feng, 1991). This makes it an important player in neuroimmune communication, and can explain why its dysfunction is implicated in many neuroinflammatory and neurodegenerative diseases (Plitman et al., 2014; Bryleva and Brundin, 2017; Ferreira et al., 2018).

First, this study showed that the LMMP-derived myenteric neuron/glia culture established by Smith et al. does indeed express NMDA receptors, and therefore should theoretically be susceptible to glutamate-induced excitotoxicity. Seeing as how excitotoxicity in the ENS is still regarded with skepticism (Gershon and Bursztajn, 1978; Kirchgessner, Liu and Alcantara, 1997) and most of the work in this area has been done in the guinea pig, this murine myenteric neuron/glia culture could provide a less expensive and easier alternative to expand research in this area.

Furthermore, as shown in Figures 9 and 10 our results indicate that murine BMMCs express both kynurenine-3-monooxygenase (*Kmo*), and kynurenine aminotransferase III (*Kat*), suggesting that both the neuroprotective and neurotoxic “arms” of the kynurenine pathway are functional. This refutes our hypothesis that BMMCs would only be able to produce the neuroprotective metabolite KYNA. Since both arms of the pathway are accessible to BMMCs further experiments will have to be conducted in order to get a clearer picture of how the kynurenine metabolism in mast cells might affect neuronal cells in excitotoxic conditions.

Currently in the literature, there is some evidence of mast cells having neurotoxic and proinflammatory effects on the ENS. For instance, some studies have correlated increased numbers of activated mast cells in close proximity to colonic nerves with higher levels of patient-reported abdominal pain and discomfort (Barbara et al., 2004; O’Sullivan et al., 2000). Furthermore, an *in vitro* study published in *Neuropharmacology* by Sand et al. in 2008 suggested that mast cells decrease neuronal survival when co-cultured with myenteric neurons. Additionally, this effect was blocked by adding protease inhibitors, a mast cell stabilizer, or a proteinase-activated receptor₂ (PAR₂) antagonist. Finally, there seems to be some evidence of decreased kynurenic acid:kynurenine ratio in males with IBS (Clarke et al., 2009), lending support to the idea that immune activation can induce IDO thereby increasing production of potentially damaging neuroactive metabolites such as QUIN (Saito, Crowley, Markey and Heyes, 1993).

Finally, this study also showed preliminary evidence of BMMCs co-cultured with LMMP-derived myenteric neurons reducing cell viability, as measured by LDH assay (Figure 11). As previously stated, further tests with LMMP-derived neurons and BMMCs in QUIN-induced excitotoxic conditions were planned but were unable to be completed due to time constraints brought on partly by the long

maturation period of BMMC cultures and their extreme sensitivity to changes in their environment. Figure 12 shows preliminary proof-of-concept data that demonstrates QUIN-induced excitotoxicity in the SK-N-SH cell line, which expresses functional NMDA receptors (Pizzi et al., 2002). Unlike in studies first performed in hippocampal slices (Boegman et al., 1985) KYNA does not seem to counteract the excitotoxic effects of QUIN in this cell line. This could be due to the fact that it is a neuroblastoma cell line, and neuroblastoma cells are known to respond differently to QUIN and KYNA, with one study suggesting that the presence of QUIN in the medium increased SK-N-SH cell viability (Guillemin et al., 2007).

This research question could have been explored in other ways, such as adding BMMC conditioned media instead of live mast cells in order to ensure that the mast cells were truly in a resting state and not in an active, degranulation state. Alternatively, live Ca^{2+} imaging could be utilized to see if the presence of BMMCs reduces excitotoxic Ca^{2+} influx in LMMP-derived myenteric neurons. This might be a more direct and accurate way of quantifying excitotoxic cell death.

Overall, using the methodology that this research project developed, future studies can further investigate the effects of excitotoxic kynurenine metabolites on nerve-mast cell interactions. Experiments building upon those discussed here could include additional immunofluorescence to stain for active caspase-3 as an additional way to classify dead cells, further work optimizing the LDH assay for the LMMP-derived myenteric neuron/glia and BMMC co-culture, and a more expensive, but more accurate measure of apoptosis, the TUNEL assay. Additionally, high performance liquid chromatography (HPLC) could be used to determine if mast cells will produce kynurenine pathway metabolites when given the precursors.

Chapter 6: Conclusions

Overall, this research demonstrated that LMMP-derived myenteric neurons appear to express NMDA receptor subtypes *Nr1*, *Nr2a*, *Nr2b*, and *Nr2c*, and BMMCs seem to express *Kmo* and *Kat*, the enzymes necessary to produce QUIN and KYNA, respectively. However, the preliminary LDH assay and immunofluorescence data suggest that production of KYNA may not be a neuroprotective measure employed by BMMCs, as evidenced by increased measures of cell death in LMMP and BMMC co-cultures.

Future studies building upon this research could use this co-culture model as a method of studying mast-nerve cell interactions in the context of visceral pain and inflammation seen in IBS. This could help further progress towards an understanding of the elusive neurophysiological basis behind this extremely prevalent disorder.

All in all, mast cell-nerve communications and the kynurenine pathway both represent very complex, interconnected systems that are likely to serve many different physiological roles. Because of the complexity of the system, a relatively controlled *in vitro* model such as the co-culture system developed in this thesis may represent an invaluable tool to further much-needed mechanistic research in this area.

Appendix

A.1 BMMC Culture Protocol (Adapted from Khambati et al., 2017)

See recipes for BMMC media and supplement below.

1. Fill a 50 mL Falcon tube with BMMC medium and place on ice.
2. Cull two Balb/c mice, collect their femurs, and place them into the medium-filled tube.
3. In a biosafety hood, use scissors and forceps to cut the ends off of the femur to expose the bone marrow.
4. Use a 25-gauge needle and 10 mL syringe, use BMMC medium to flush the bone marrow out of the femur and into a clean 50 mL Falcon tube, and repeat for the remaining femurs the bone should turn white when all of the bone marrow has been flushed out.
5. Centrifuge the bone marrow at 1200 rpm for 10 minutes.
6. Re-suspend the cells in 10 mL of BMMC medium.
7. Strain the solution through a 45 μm cell strainer (VWR) to remove the excess fat/muscle tissue.
8. Count the cells using a 10x dilution in Trypan blue (Gibco).
9. Add BMMC media to adjust the concentration to 2.0×10^6 cells/mL.
10. Add 2 mL of suspended cells to 18 mL of BMMC media into 75 cm^2 cell culture flasks for a final concentration of 2.0×10^5 cells/mL.
11. Incubate the flasks at 37 °C in a 5% CO_2 humidified atmosphere.
12. Change flasks every 6-7 days.
13. BMMCs are ready for use after 4 weeks.

BMMC Media:

- 500 mL RPMI 1640 media (Gibco) (discard 86 mL to make 500 mL of complete media)
- 500 μL 250 $\mu\text{g/mL}$ Amphotericin- β (Gibco)
- 400 μL of 1 mM recombinant mouse SCF solution in deionized H_2O
- 400 μL of 1 mM recombinant mouse SCF solution in deionized H_2O
- 50 mL Fetal Bovine Serum (Gibco)
- 5 mL of 10,000 U/mL Pen Strep (Gibco)
- 30 mL of BMMC supplement (see below)

BMMC Supplement:

- 29 μL β -mercaptoethanol
- 3 mL of 200 mM L-glutamine (Gibco)

- 5 mL 20x MEM NEAA (Gibco)
- Topped to 500 mL with sterile deionized H₂O

Make 30 mL aliquots and store at -20 °C until use.

A.2 LMMP Culture Protocol (Adapted from Smith et al., 2013)

Complete advance preparation instructions below before starting the culture protocol.

1. Gather clean (preferably sterile) surgical materials and tools. You will need small scissors, angled forceps, cotton swabs, three clean 200 mL glass beakers, 10 mL syringes, and a dark-coloured glass or plastic rod (a small paintbrush works perfectly).
2. Put Krebs solution on ice and bubble with carbogen for 30 minutes.
3. Label the three 200 mL beakers “dirty”, “clean”, and “LMMP”, and keep the LMMP beaker placed on ice and bubbling with carbogen.
4. Euthanize the male 6-8-week-old Swiss Webster mouse by cervical dislocation. Place the mouse with its abdomen upright on the surgical surface.
5. Clean the skin using 70% ethanol, lift the abdominal skin using forceps, and use scissors to cut the skin to reveal the abdominal cavity and the gut.
6. Remove the length of the gastrointestinal tract gently with forceps and use scissors to collect the ileum by cutting an approximately 10 cm long section of ileum distal to the stomach and proximal to the caecum.
7. Place the entire ileum into the Krebs-filled beaker labeled “dirty”.
8. Repeat steps 4-7 with the second mouse (it is better to cull one mouse at a time because the LMMP tissue dies of hypoxia very quickly).
9. Cut off the wide end of a 20-200 μ L pipette tip with blunt scissors and attach it to a 10 mL syringe to create a tool to flush the ileum.
10. Cut each ileum into 2-3 large pieces. Gently stick the tool into each piece and flush out the intestinal contents with Krebs solution into a waste beaker. Place the cleaned ileum into the beaker labeled “clean”. Repeat this process for each section of ileum.
11. Cut the clean ileum sections into smaller, 2-4 cm pieces. Cannulate a segment onto a clean paintbrush or rod and prevent the intestine from rotating by gently pinning it down using the thumb.
12. To harvest the LMMP, gently run the edge of the angled forceps down the length of the cannulated ileum to make a linear indent. Then, using a Krebs soaked cotton swab, gently tease the muscle layer towards the line using small horizontal strokes. Do this along the entire length of the segment and the LMMP should start to separate from the circular muscle. Finally, using angled forceps, strip the LMMP tissue from the ileum gently from top to bottom.
13. Place the LMMP into the beaker filled with carbogen-bubbling Krebs solution. Repeat until all of the LMMP from each of the segments has been harvested.
14. To avoid any contamination, rinse the LMMP tissue three times by filling three 1.5 mL Eppendorf tubes with 0.5 mL Krebs labeled “1”, “2”, and “3”. Gather the LMMP in the beaker by swirling and collecting LMMP

with fine, pointed forceps, and all of the tissue into the Eppendorf labeled “1”.

15. Spin the first Eppendorf for 30 seconds at 4 °C on low speed (356 x g) to avoid damaging the tissue. Using fine-tipped forceps, transfer the pellet to the next tube and repeat this process for each remaining tube.
16. Once the tissue has been rinsed, prepare the digestion solution by dissolving 3 mg of bovine serum albumin (BSA) (Sigma) and 13 mg of collagenase type 2 into a 50 mL Falcon tube containing 10 mL of bubbled Krebs solution.
17. Carefully remove LMMP pellet and place (along with 1 mL of Krebs) onto a small petri dish. Use fine scissors to snip the tissue into tiny pieces. Use a transfer pipette to put the tissue into the Falcon tube containing the digestion solution.
18. Digest the LMMP for 1 hour in a 37 °C water bath bubbled with carbogen. (Make sure the carbogen is at a very low pressure so that too many bubbles don't occur and carry the small pieces of LMMP out of the tube).
19. Gather the cells via centrifugation for 8 minutes at 356 x g in a centrifuge cooled to 4 °C.
20. From this point forward all steps should take place in a sterile cell culture hood environment. All reagents and tools used should be sterilized before use!
21. During centrifugation prepare a sterile 0.05% trypsin solution in a new 50 mL Falcon HBSS by placing 1 mL of warmed 0.25% trypsin in 4 mL of warmed HBSS.
22. After centrifugation, remove and discard the supernatant.
23. Carefully transfer the pellet into the digestion solution using a transfer pipette.
24. Digest LMMP in a gently shaking 37 °C water bath for 7 minutes. Do not exceed 7 minutes or the neurons will die.
25. Neutralize the trypsin by adding 5 mL of ENC media to the tube.
26. Gather the cells via centrifugation for 8 minutes at 356 x g in a centrifuge cooled to 4 °C. Carefully remove and discard all of the supernatant with a transfer pipette.
27. Gently re-suspend the pellet in 5 mL of ENC media. Try not to create bubbles.
28. Balance a piece of Nitrex mesh on top of a sterile 15 mL Falcon tube.
29. Using a transfer pipette, transfer the suspended cells into the Falcon tube through the mesh.
30. Cap the tube and place it in a Hula mixer in 4 °C with gentle rolling and tilting for 30 minutes.
31. Gather the cells via centrifugation for 8 minutes at 356 x g in a centrifuge cooled to 4 °C. Carefully remove and discard all of the supernatant with a transfer pipette.

32. Resuspend the cells in 1300 μL of ENC media and mix the cells gently by pipetting up and down with a 20-200 μL pipette tip. Try not to generate air bubbles
33. Add 750 μL of ENC media and 100 μL of cells to each of the wells containing the pre-coated glass coverslips.
34. Incubate plates in a cell culture incubator at 37 $^{\circ}\text{C}$ in a humidified atmosphere with 5% CO_2 .
35. Change half of the cell media every 2 days.

Preparation of Sterile Coated Glass Coverslip Plates

Preparation of plates can be done up to 2 weeks in advance of the LMMP culture. Coated plates should be stored protected from light at 4 $^{\circ}\text{C}$. This procedure should be performed in sterile conditions in a biosafety cabinet and all tools and reagents used in this procedure should be sterilized via autoclave before-hand.

1. In a biosafety hood use sterile fine-tipped forceps to place autoclaved circular glass coverslips (one per well) into 12 wells in the 24-well plate.
2. (Although Smith et al. used poly-D lysine, we used poly-L-lysine due to availability. This did not seem to affect laminin adherence).
3. Pipette 450 μL of poly-L-lysine solution onto the glass coverslips inside the 24-well plate. Let the solution settle for at least 10 minutes.
4. Aspirate the poly-L-lysine solution and rinse coverslips 3x with sterile deionized water.
5. Allow plates to dry for at least 2 hours inside the biosafety cabinet. Once dry, the plates may be stored at either 4 $^{\circ}\text{C}$ or -20 $^{\circ}\text{C}$ before laminin coating.
6. Prepare laminin stock ahead of time by thawing it on ice and diluting it to a concentration of 50 $\mu\text{g}/\text{mL}$. Store aliquots at -80 $^{\circ}\text{C}$. Thaw the aliquots on ice before use.
7. To coat the coverslips with laminin, pipette 450 μL of laminin solution into each well.
8. Incubate the laminin solution on the coverslips for 1 hour.
9. Aspirate the laminin solution without disturbing the coverslips and rinse the coverslips once with sterile deionized water.
10. Briefly let the plates dry and store the plates (make sure to keep them sterile) at 4 $^{\circ}\text{C}$ for up to 2 weeks before use.

Enteric Neuron Media

Prepare 50 mL of complete enteric neuron media and sterilize it in advance with a 0.2 μm bottle-top filter (VWR). Store at 4 $^{\circ}\text{C}$ until use.

- 47.5 mL Neurobasal A media (Gibco)
- 1 mL B-27 Plus Supplement (50x) (Thermofisher Scientific)
- 500 μ L Fetal Bovine Serum (Gibco)
- 500 μ L 200 mM L-glutamine (Gibco)
- 500 μ L Antibiotic/Antimycotic 100x liquid (Gibco)
- 50 μ L of 10 μ g/mL Glial-Derived Neurotrophic Factor (GDNF) (PeproTech) stock solution in sterile deionized water (store GDNF stock in 50 μ L aliquots at -20 °C until use).

Krebs Solution

Prepare 1 L of Krebs solution and sterilize it in advance with a 0.2 μ m bottle-top filter (VWR). Store at 4 °C until use for no longer than two weeks. Final concentrations of reagents are shown in parentheses. Add the following reagents to 1 L of deionized water while stirring:

- 6.9 g NaCl (118 mM)
- 0.343 g KCl (4.6 mM)
- 0.156 g NaH₂PO₄ (1.3 mM)
- 0.1445 g MgSO₄ (1.2 mM)
- 2.1 g NaHCO₃ (25 mM)
- 1.98 g glucose (11 mM)
- 0.278 g CaCl₂ (2.5 mM)

Before starting the experiment, make sure to stabilize the pH of the Krebs solution by bubbling it with 5% carbogen for 30 minutes.

A.3 CellProfiler Pipeline

Pipeline Outline

Modules that are italicized are used for calibration only, and not in the final analysis.

Modules denoted with a (*) have defined parameters and settings shown in the tables below.

Repeated modules are indicative of an analysis that was run on images from each colour channel.

1. Images
2. Metadata
3. Names and Types
4. Groups
5. Identify Primary Objects*
6. Identify Primary Objects*
7. *Measure Object Size and Shape*
8. Measure Object Intensity*
9. Measure Object Intensity*
10. *Overlay Outlines*
11. *Overlay Outlines*
12. *Display Data on Image*
13. *Display Data on Image*
14. *Display Histogram*
15. *Display Histogram*
16. *Classify Objects*
17. *Classify Objects*
18. Filter Objects*
19. Filter Objects*
20. Relate Objects*
21. Filter Objects*
22. *Display Data on Image*
23. *Calculate Math*
24. Export to Spreadsheet

Module Functions

Images

Allows the user to specify the location of image files for the program to analyze. It also allows the user to filter images by a variety of criteria, including file extension, file location, and file name.

Metadata

Allows the user to extract information from the metadata of the inputted images. This data will then be sorted and displayed along with the measurement data.

Names and Types

The Names and Types module allows the user to give groups of images meaningful names and define whether an image set should be processed as 2 dimensional or 3 dimensional. Subsequent modules will refer to the images by these names.

Groups

The Groups module allows the investigator to split the images into groups, which will be processed independently of each other.

Identify Primary Objects*

This module uses parameters inputted by the user to identify biological objects of interest. In order to work properly, it requires grayscale images containing light objects on a dark background.

Measure Object Size and Shape

This module can be used to measure several geometric features of the identified objects. This data was required to ensure the accuracy of the Identify Primary Objects module, since it uses size to discriminate between objects.

Measure Object Intensity

When given an image with identified objects, this module extracts intensity measurements for each object based on one or more corresponding grayscale images.

Overlay Outlines

This module puts outlines of identified objects on any desired image. The resulting image can be saved using the Save Images module. This module was very helpful for visualizing the data in the early phases of the pipeline design.

Display Data on Image

This module produces an image labeled with measured data that appears on top of identified objects. This module was very helpful for visualizing the data in the early phases of the pipeline design.

Display Histogram

This module plots a histogram of the desired measurement data. This module was very helpful for visualizing the data in the early phases of the pipeline design.

Classify Objects

This module classifies identified objects into different categories according to the values of the measurements chosen by the investigator. Since the output of this module is histograms with counts of objects in each group, this module was useful in testing parameters during the trial and error phase of designing the pipeline.

*Filter Objects**

This module eliminates objects based on a specified measurement. The first sets of filtering were used to set an intensity threshold which designates whether or not an object that has been identified is a neuron or not, and whether or not an object is dead or not. The specific thresholds for what constitutes a neuron or what constitutes a dead cell were decided by choosing the lower quartile mean intensity as the threshold. This means that the cut-off can be consistent throughout different batches of slides, while still keeping the threshold relevant to the specific dataset.

*Relate Objects**

This module allows the user to associate one type of object with another type of object. The object that is assigned is called the child object, and the object to which something is assigned is called the parent object. In this pipeline, we were trying to count the number of cells that are both neurons (stained with β -III tubulin) and are also dead (stained with propidium iodide). The parent was chosen as the neurons which meet the threshold from the previous module, while the children were chosen as the dead cells which meet the threshold set by the previous module. The method by which the program calculated the distance to the child objects is called the centroid method. This method finds the closest nearby child objects as measured from centre point of the parent object.

*Filter Objects 2**

The second set of filtering is to exclude all of the objects that both are not within the intensity threshold and/or do not have a related object from the previous

module. This excludes every object except for those that are stained for β -III-tubulin and propidium iodide, and also have these two stains overlapping.

Display Data on Image

This module produces an image with measured data on top of the identified objects. It was used to display dead and live neuron counts on individual images so that the automated analysis could be easily compared to manual counts done by the investigator.

Calculate Math

This module was used to calculate the percentage of live neurons identified by the previous modules. This was calculated by taking the ratio of dead neurons to total neurons. More detailed calculations were processed in Excel after, but this allows the user to quickly see the results.

Export to Spreadsheet

This module exports selected data from the analysis and creates a spreadsheet in Excel. From there the data could be analysed in more detail.

Parameters and Settings

Table A3.1: Identify Primary Objects (ENC Neurons)

Parameter	Setting
Use advanced settings?	Yes
Typical diameter of objects in pixel units (Min, Max)	24,44
Discard objects outside of parameter range?	Yes
Discard objects touching the border of the image?	No
Threshold strategy	Adaptive
Thresholding method	Otsu
Two or three class thresholding?	Two classes
Threshold smoothing scale	1.3488
Threshold correction factor	1.1
Lower and upper bounds on threshold	0.0,1.0
Size of adaptive window	24
Method to distinguish clumped objects	Shape
Method to draw dividing lines between	Propagate

objects	
Automatically calculate size of smoothing filter for declumping?	Yes
Automatically calculate minimum allowed distance between local maxima?	Yes
Speed up by using lower resolution image to find local maxima?	No
Fill holes in identified objects?	After declumping only
Handling if excessive number of objects identified	Continue

Table A3.2: Identify Primary Objects (ENC Dead Cells)

Parameter	Setting
Use advanced settings?	Yes
Typical diameter of objects in pixel units (Min, Max)	24,44
Discard objects outside of parameter range?	Yes
Discard objects touching the border of the image?	No
Threshold strategy	Adaptive
Thresholding method	Otsu
Two or three class thresholding?	Two classes
Threshold smoothing scale	1.3488
Threshold correction factor	1.1
Lower and upper bounds on threshold	0.0,1.0
Size of adaptive window	24
Method to distinguish clumped objects	Shape
Method to draw dividing lines between objects	Propagate
Automatically calculate size of smoothing filter for declumping?	No
Size of smoothing filter	10
Automatically calculate minimum allowed distance between local maxima?	Yes
Speed up by using lower resolution image to find local maxima?	No
Fill holes in identified objects?	After declumping only
Handling if excessive number of objects identified	Continue

Table A3.3: Filter Objects (Neurons Intensity)

Parameter	Setting
Select the filtering mode	Measurements
Select the filtering method	Limits
Select the measurement to filter by	Category: Intensity Measurement: Mean Intensity
Filter using a minimum measurement value?	Yes
Minimum value	0.09
Filter using a maximum measurement value?	No

Table A4: Filter Objects (Dead Cells Intensity)

Parameter	Setting
Select the filtering mode	Measurements
Select the filtering method	Limits
Select the measurement to filter by	Intensity
Filter using a minimum measurement value?	Mean Intensity
Minimum value	0.22
Filter using a maximum measurement value?	No

Table A5: Relate Objects

Parameter	Setting
Parents Objects	Neurons intensity
Child Objects	Dead intensity
Calculate child-parent distances?	Centroid
Calculate distances to other parents?	No

Table A6: Filter Objects (Neurons Intensity by Dead Cells Intensity)

Parameter	Setting
Select the objects to filter	Neurons intensity
Select the filtering mode	Measurements
Select the filtering method	Limits

Select the measurement to filter by	Category: Children Measurement: Count
Filter using a minimum measurement value?	Yes
Minimum value	1
Filter using a maximum measurement value?	No

Bibliography

1. Azbill, R. D., Mu, X., Bruce-Keller, A. J., Mattson, M. P., & Springer, J. E. (1997). Impaired mitochondrial function, oxidative stress and altered antioxidant enzyme activities following traumatic spinal cord injury. *Brain Research*, 765(2). [https://doi.org/10.1016/S0006-8993\(97\)00573-8](https://doi.org/10.1016/S0006-8993(97)00573-8)
2. Barbara, G., Stanghellini, V., De Giorgio, R., Cremon, C., Cottrell, G.S., Santini, D., Pasquinelli, G., Morselli-Labate, A.M., Grady, E.F., Bunnett, N.W., Collins, S.M., and Corinaldesi, R., 2004. Activated Mast Cells in Proximity to Colonic Nerves Correlate with Abdominal Pain in Irritable Bowel Syndrome. *Gastroenterology*, [online] 126(3), pp.693–702.
3. Bauer, O., and Razin, E., 2000. Mast Cell-Nerve Interactions. *Physiology*, [online] 15(5), pp.213–218.
4. Berger, M., Gray, J.A., and Roth, B.L., 2009. The Expanded Biology of Serotonin. *Annual Review of Medicine*, [online] 60(1), pp.355–366.
5. Bian, X., Zhou, X., & Galligan, J. J. (2004). R-type calcium channels in myenteric neurons of guinea pig small intestine. *American Journal of Physiology - Gastrointestinal and Liver Physiology*, 287(1).
6. Boegman, R. J., El-Defrawy, S. R., Jhamandas, K., Beninger, R. J., & Ludwin, S. K. (1985). Quinolinic acid neurotoxicity in the nucleus basalis antagonized by kynurenic acid. *Neurobiology of Aging*, 6(4). [https://doi.org/10.1016/0197-4580\(85\)90012-0](https://doi.org/10.1016/0197-4580(85)90012-0)
7. Boegman, R.J., El-Defrawy, S.R., Jhamandas, K., Beninger, R.J., and Ludwin, S.K., 1985. Quinolinic acid neurotoxicity in the nucleus basalis antagonized by kynurenic acid. *Neurobiology of Aging*, [online] 6(4), pp.331–336.
8. Braidy, N., Grant, R., Adams, S., Brew, B. J., & Guillemin, G. J. (2009). Mechanism for quinolinic acid cytotoxicity in human astrocytes and neurons. *Neurotoxicity Research*, 16(1). <https://doi.org/10.1007/s12640-009-9051-z>
9. Bryleva, E. Y., & Brundin, L. (2017, January). Kynurenine pathway metabolites and suicidality. *Neuropharmacology*, Vol. 112. <https://doi.org/10.1016/j.neuropharm.2016.01.034>
10. Bryleva, E.Y., and Brundin, L., 2017. Kynurenine pathway metabolites and suicidality. *Neuropharmacology*, [Accessed 30 Jul. 2018].
11. Burns, G.A., and Stephens, K.E., 1995. Expression of mRNA for the N-methyl-d-aspartate (NMDAR1) receptor and vasoactive intestinal polypeptide (VIP) co-exist in enteric neurons of the rat. *Journal of the Autonomic Nervous System*, [online] 55(3), pp.207–210.
12. Campbell, B.M., Charych, E., Lee, A.W., and Möller, T., 2014. Kynurenines in CNS disease: regulation by inflammatory cytokines. *Frontiers in Neuroscience*, [online] 8, p.12.
13. Chey, W.D., Kurlander, J., and Eswaran, S., 2015. Irritable Bowel Syndrome. *JAMA*, [online] 313(9), p.949.

14. Choi, D. W. (2017). Excitotoxicity and Stroke. In *Primer on Cerebrovascular Diseases: Second Edition*. <https://doi.org/10.1016/B978-0-12-803058-5.00048-5>
15. Clapham, D. E. (2007). Calcium Signaling. *Cell*, 131(6). <https://doi.org/10.1016/j.cell.2007.11.028>
16. Clarke, G., Fitzgerald, P., Cryan, J.F., Cassidy, E.M., Quigley, E.M., and Dinan, T.G., 2009. Tryptophan degradation in irritable bowel syndrome: Evidence of indoleamine 2,3-dioxygenase activation in a male cohort. *BMC Gastroenterology*, [online] 9, p.6.
17. Cruz, V. P. D. la, Carrillo-Mora, P., & Santamaría, A. (2013). Quinolinic acid, an endogenous molecule combining excitotoxicity, oxidative stress and other toxic mechanisms. *International Journal of Tryptophan Research*, Vol. 5. <https://doi.org/10.4137/IJTR.S8158>
18. Darlington, L. G., Forrest, C. M., Mackay, G. M., Smith, R. A., Smith, A. J., Stoy, N., & Stone, T. W. (2010). On the Biological Importance of the 3-hydroxyanthranilic Acid: Anthranilic Acid Ratio. *International Journal of Tryptophan Research: IJTR*, 3.
19. Edvinsson, L., Cervós-Navarro, J., Larsson, L.I., Owman, C.H., and Rönnberg, A.L., 1977. Regional distribution of mast cells containing histamine, dopamine, or 5-hydroxytryptamine in the mammalian brain. *Neurology*, [online] 27(9), pp.878–883.
20. Espey, M. G., Chernyshev, O. N., Reinhard, J. F., Namboodiri, M. a, & Colton, C. a. (1997). Activated human microglia produce the excitotoxin quinolinic acid. *Neuroreport*, 8(2). <https://doi.org/10.1097/00001756-199701200-00011>
21. Ferreira, F.S., Biasibetti-Brendler, H., Pierozan, P., Schmitz, F., Bertó, C.G., Prezzi, C.A., Manfredini, V., and Wyse, A.T.S., 2018. Kynurenic Acid Restores Nrf2 Levels and Prevents Quinolinic Acid-Induced Toxicity in Rat Striatal Slices. *Molecular Neurobiology*, [online] 21 Mar., pp.1–12.
22. Forsythe, P. (2019). Mast Cells in Neuroimmune Interactions. *Trends in Neurosciences*, 42(1). <https://doi.org/10.1016/j.tins.2018.09.006>
23. Forsythe, P., & Bienenstock, J. (2012). The mast cell- nerve functional unit: A key component of physiologic and pathophysiologic responses. In *Allergy and the Nervous System (Vol. 98)*. <https://doi.org/10.1159/000336523>
24. Forsythe, P., and Bienenstock, J., 2012. The mast cell- nerve functional unit: A key component of physiologic and pathophysiologic responses. In: *Allergy and the Nervous System*. [online] Karger Publishers, pp.196–221.
25. Furness, J. Barton. (2006). *The enteric nervous system* (p. 274). Blackwell Pub.
26. Galligan, J. J., LePard, K. J., Schneider, D. A., & Zhou, X. (2000). Multiple mechanisms of fast excitatory synaptic transmission in the enteric nervous system. *Journal of the Autonomic Nervous System*, 81(1–3).
27. GAMBLE, H. J., & GOLDBY, S. (1961). Mast Cells in Peripheral Nerve Trunks. *Nature*, 189(4766). <https://doi.org/10.1038/189766a0>

28. Gershon, M.D., and Bursztajn, S., 1978. Properties of the enteric nervous system: Limitation of access of intravascular macromolecules to the myenteric plexus and muscularis externa. *The Journal of Comparative Neurology*, [online] 180(3), pp.467–487.
29. Guillemin, G. J. (2012). Quinolinic acid, the inescapable neurotoxin. *FEBS Journal*, 279(8). <https://doi.org/10.1111/j.1742-4658.2012.08485.x>
30. Guillemin, G. J., Smythe, G., Takikawa, O., & Brew, B. J. (2005). Expression of indoleamine 2,3-dioxygenase and production of quinolinic acid by human microglia, astrocytes, and neurons. *GLIA*, 49(1). <https://doi.org/10.1002/glia.20090>
31. Guillemin, G.J., Cullen, K.M., Lim, C.K., Smythe, G.A., Garner, B., Kapoor, V., Takikawa, O., and Brew, B.J., 2007. Characterization of the kynurenine pathway in human neurons. *J Neurosci*, 27(47), pp.12884–12892.
32. Hagiwara, M., Furuno, T., Hosokawa, Y., Iino, T., Ito, T., Inoue, T., ... Ito, A. (2011). Enhanced Nerve-Mast Cell Interaction by a Neuronal Short Isoform of Cell Adhesion Molecule-1. *The Journal of Immunology*, 186(10). <https://doi.org/10.4049/jimmunol.1002244>
33. Hu, H. Z., Ren, J., Liu, S., Gao, C., Xia, Y., & Wood, J. D. (1999). Functional group I metabotropic glutamate receptors in submucous plexus of guinea-pig ileum. *British Journal of Pharmacology*, 128(8). <https://doi.org/10.1038/sj.bjp.0702980>
34. Hughes, J. R. (2009). Alcohol withdrawal seizures. *Epilepsy & Behavior*, 15(2). <https://doi.org/10.1016/j.yebeh.2009.02.037>
35. Jaiswal, M., Zech, W. D., Goos, M., Leutbecher, C., Ferri, A., Zippelius, A., ... Keller, B. U. (2009). Impairment of mitochondrial calcium handling in a mtSOD1 cell culture model of motoneuron disease. *BMC Neuroscience*, 10(1). <https://doi.org/10.1186/1471-2202-10-64>
36. JONAS, S., SUGIMORI, M., & LLINÁS, R. (1997). Is Low Molecular Weight Heparin a Neuroprotectant? *Annals of the New York Academy of Sciences*, 825(1 Neuroprotecti). <https://doi.org/10.1111/j.1749-6632.1997.tb48449.x>
37. Kennedy, P. J. J., Cryan, J. F. F., Dinan, T. G. G., & Clarke, G. (2017). Kynurenine pathway metabolism and the microbiota-gut-brain axis. *Neuropharmacology*, 112(Pt B). <https://doi.org/10.1016/j.neuropharm.2016.07.002>
38. Khambati, I., Han, S., Pijnenburg, D., Jang, H., & Forsythe, P. (2017). The bacterial quorum-sensing molecule, N-3-oxo-dodecanoyl-l-homoserine lactone, inhibits mediator release and chemotaxis of murine mast cells. *Inflammation Research*, 66(3). <https://doi.org/10.1007/s00011-016-1013-3>
39. Kim, D.-Y., and Camilleri, M., (2000). Serotonin: a mediator of the brain-gut connection. *The American Journal of Gastroenterology*, [online] 95(10), pp.2698–2709.

40. Kirchgessner, A. L., Liu, M. T., & Alcantara, F. (1997). Excitotoxicity in the enteric nervous system. *The Journal of Neuroscience: The Official Journal of the Society for Neuroscience*, 17(22).
41. Kitamura, Y. et al. (1987) Mutual phenotypic changes between connective tissue type and mucosal mast cells. *International Archives of Allergy and Immunology*, 82, 244–248.
42. Kumar, V., and Sharma, A., (2010). Mast cells: Emerging sentinel innate immune cells with diverse role in immunity. *Molecular Immunology*, Available at: <<http://www.ncbi.nlm.nih.gov/pubmed/20678798>> [Accessed 23 Jan. 2018].
43. Leigh, P. N., & Meldrum, B. S. (1987). American Academy of Neurology. 39th annual meeting program. New York, New York, April 5-11, 1987. Abstracts. *Neurology*, 37(3 Suppl 1). https://doi.org/10.1212/wnl.47.6_suppl_4.221s
44. Leon, A., Burianni, A., Dal Toso, R., Fabris, M., Romanello, S., Aloe, L., & Levi-Montalcini, R. (1994). Mast cells synthesize, store, and release nerve growth factor. *Proceedings of the National Academy of Sciences*, 91(9). <https://doi.org/10.1073/pnas.91.9.3739>
45. Li, Z. S., Pham, T. D., Tamir, H., Chen, J. J., & Gershon, M. D. (2004). Enteric Dopaminergic Neurons: Definition, Developmental Lineage, and Effects of Extrinsic Denervation. *Journal of Neuroscience*, 24(6). <https://doi.org/10.1523/JNEUROSCI.3982-03.2004>
46. Lim, C.K., Fernández-Gomez, F.J., Braidy, N., Estrada, C., Costa, C., Costa, S., Bessede, A., Fernandez-Villalba, E., Zinger, A., Herrero, M.T., and Guillemin, G.J., 2017. Involvement of the kynurenine pathway in the pathogenesis of Parkinson's disease. *Progress in Neurobiology*, [online] 155, pp.76–95.
47. Liu, M. T., Rothstein, J. D., Gershon, M. D., & Kirchgessner, A. L. (1997). Glutamatergic enteric neurons. *The Journal of Neuroscience: The Official Journal of the Society for Neuroscience*, 17(12).
48. Lopez-Ibor, J.J.J., 1992. Serotonin and psychiatric disorders. *International clinical psychopharmacology*, [online] 7 Suppl 2, pp.5–11.
49. Lugo-Huitrón, R., Ugalde Muñiz, P., Pineda, B., Pedraza-Chaverri, J., Ríos, C., & Pérez-de la Cruz, V. (2013). Quinolinic acid: an endogenous neurotoxin with multiple targets. *Oxidative Medicine and Cellular Longevity*, 2013. <https://doi.org/10.1155/2013/104024>
50. M. Flint Beal. (1998). Excitotoxicity and nitric oxide in parkinson's disease pathogenesis. *Annals of Neurology*, 44(S1). <https://doi.org/10.1002/ana.410440716>
51. Manev, H., Favaron, M., Guidotti, A., & Costa, E. (1989). Delayed increase of Ca²⁺ influx elicited by glutamate: role in neuronal death. *Molecular Pharmacology*, 36(1).
52. Martinucci, I., Blandizzi, C., de Bortoli, N., Bellini, M., Antonioli, L., Tuccori, M., ... Colucci, R. (2015). Genetics and pharmacogenetics of

- aminergic transmitter pathways in functional gastrointestinal disorders. *Pharmacogenomics*, 16(5). <https://doi.org/10.2217/pgs.15.12>
53. Molinuevo, J. L., Lladó, A., & Rami, L. (2005). Memantine: Targeting glutamate excitotoxicity in Alzheimer's disease and other dementias. *American Journal of Alzheimer's Disease & Other Dementias*, 20(2). <https://doi.org/10.1177/153331750502000206>
54. Newson, B., Dahlström, A., Enerbäck, L., & Ahlman, H. (1983). Suggestive evidence for a direct innervation of mucosal mast cells: An electron microscopic study. *Neuroscience*, 10(2). [https://doi.org/10.1016/0306-4522\(83\)90153-7](https://doi.org/10.1016/0306-4522(83)90153-7)
55. O'Mahony, S. M., Clarke, G., Borre, Y. E., Dinan, T. G., & Cryan, J. F. (2015). Serotonin, tryptophan metabolism and the brain-gut-microbiome axis. *Behavioural Brain Research*, 277. <https://doi.org/10.1016/J.BBR.2014.07.027>
56. O'Sullivan, Clayton, Breslin, Harman, Bountra, McLaren, and O'Morain, 2000. Increased mast cells in the irritable bowel syndrome. *Neurogastroenterology and Motility*, [online] 12(5), pp.449–457.
57. Otsu, N., 1979. A Threshold Selection Method from Gray-Level Histograms. *IEEE Transactions on Systems, Man, and Cybernetics*, [online] 9(1), pp.62–66.
58. Oxenkrug, G. F. (2010). Tryptophan kynurenine metabolism as a common mediator of genetic and environmental impacts in major depressive disorder: the serotonin hypothesis revisited 40 years later. *The Israel Journal of Psychiatry and Related Sciences*, 47(1). <https://doi.org/10.1016/j.neulet.2010.11.003>. Melatonin
59. Paré, P., Gray, J., Lam, S., Balshaw, R., Khorasheh, S., Barbeau, M., Kelly, S., and McBurney, C.R., 2006. Health-related quality of life, work productivity, and health care resource utilization of subjects with irritable bowel syndrome: Baseline results from logic (longitudinal outcomes study of gastrointestinal symptoms in Canada), a naturalistic study. *Clinical Therapeutics*, [online] 28(10), pp.1726–1735. [/article/abs/pii/S0149291806002505](https://doi.org/10.1016/j.clinther.2006.10.003) [Accessed 2 Sep. 2019].
60. Pitt, D., Werner, P., & Raine, C. S. (2000). Glutamate excitotoxicity in a model of multiple sclerosis. *Nature Medicine*, 6(1). <https://doi.org/10.1038/71555>
61. Pizzi, M., Boroni, F., Bianchetti, A., Moraitis, C., Sarnico, I., Benarese, M., Goffi, F., Valerio, A., and Spano, P., 2002. Expression of functional NR1/NR2B-type NMDA receptors in neuronally differentiated SK-N-SH human cell line. *European Journal of Neuroscience*, [online] 16(12), pp.2342–2350.
62. Plitman, E., Nakajima, S., de la Fuente-Sandoval, C., Gerretsen, P., Chakravarty, M.M., Kobylanskii, J., Chung, J.K., Caravaggio, F., Iwata, Y., Remington, G., and Graff-Guerrero, A., 2014. Glutamate-mediated excitotoxicity in schizophrenia: A review. *European Neuropsychopharmacology*, Available at:

- <<http://www.ncbi.nlm.nih.gov/pubmed/25159198>> [Accessed 6 Mar. 2018].
63. Reed, D.E., Barajas-Lopez, C., Cottrell, G., Velazquez-Rocha, S., Dery, O., Grady, E.F., Bunnett, N.W., and Vanner, S.J., 2003. Mast cell tryptase and proteinase-activated receptor 2 induce hyperexcitability of guinea-pig submucosal neurons. *The Journal of physiology*, [online] 547 (Pt 2), pp.531–42.
 64. Reis, H. J., Massensini, A. R., Prado, M. A. M., Gomez, R. S., Gomez, M. V., & Romano-Silva, M. A. (2000). Calcium channels coupled to depolarization-evoked glutamate release in the myenteric plexus of guinea-pig ileum. *Neuroscience*, 101(1). [https://doi.org/10.1016/S0306-4522\(00\)00354-7](https://doi.org/10.1016/S0306-4522(00)00354-7)
 65. Rivera, J. (2006). Snake bites and bee stings: the mast cell strikes back. *Nature Medicine*, 12(9). <https://doi.org/10.1038/nm0906-999>
 66. Saito, K., Crowley, J.S., Markey, S.P., and Heyes, M.P., 1993. A mechanism for increased quinolinic acid formation following acute systemic immune stimulation. *The Journal of biological chemistry*, [online] 268(21), pp.15496–503.
 67. Saito, Y.A., Schoenfeld, P., and Locke, G.R., (2002). The epidemiology of irritable bowel syndrome in North America: A systematic review. *American Journal of Gastroenterology*, Available at: <<http://www.nature.com/doi/10.1111/j.1572-0241.2002.05913.x>> [Accessed 2 Sep. 2019].
 68. Smith, T. H., Ngwainmbi, J., Grider, J. R., Dewey, W. L., & Akbarali, H. I. (2013). An in-vitro preparation of isolated enteric neurons and glia from the myenteric plexus of the adult mouse. *Journal of Visualized Experiments : JoVE*, (78). <https://doi.org/10.3791/50688>
 69. Suzuki, A., Suzuki, R., Furuno, T., Teshima, R., & Nakanishi, M. (2004). N-cadherin plays a role in the synapse-like structures between mast cells and neurites. *Biological & Pharmaceutical Bulletin*, 27(12). <https://doi.org/10.1248/bpb.27.1891>
 70. Tabrizi, S. J., Cleeter, M. W. J., Xuereb, J., Taanman, J.-W., Cooper, J. M., & Schapira, A. H. v. (1999). Biochemical abnormalities and excitotoxicity in Huntington's disease brain. *Annals of Neurology*, 45(1). [https://doi.org/10.1002/1531-8249\(199901\)45:1<25::AID-ART6>3.0.CO;2-E](https://doi.org/10.1002/1531-8249(199901)45:1<25::AID-ART6>3.0.CO;2-E)
 71. Taylor, M.W., and Feng, G.S., 1991. Relationship between interferon-gamma, indoleamine 2,3-dioxygenase, and tryptophan catabolism. *FASEB journal : official publication of the Federation of American Societies for Experimental Biology*, [online] 5(11), pp.2516–22.
 72. Wang, G.-D., Wang, X.-Y., Xia, Y., & Wood, J. D. (2014). Dietary Glutamate: Interactions With the Enteric Nervous System. *Journal of Neurogastroenterology and Motility*, 20(1). <https://doi.org/10.5056/jnm.2014.20.1.41>

73. Werner, C., & Engelhard, K. (2007). Pathophysiology of traumatic brain injury. *British Journal of Anaesthesia*, 99(1). <https://doi.org/10.1093/bja/aem131>
74. Wiley, J. W., Lu, Y. X., & Owyang, C. (1991). Evidence for a glutamatergic neural pathway in the myenteric plexus. *American Journal of Physiology-Gastrointestinal and Liver Physiology*, 261(4). <https://doi.org/10.1152/ajpgi.1991.261.4.G693>
75. Wilhelm, M., Silver, R., & Silverman, A. J. (2005). Central nervous system neurons acquire mast cell products via transgranulation. *European Journal of Neuroscience*, 22(9). <https://doi.org/10.1111/j.1460-9568.2005.04429.x>
76. Wong, G.W., Zhuo, L., Kimata, K., Lam, B.K., Satoh, N., and Stevens, R.L., 2014. Ancient origin of mast cells. *Biochemical and Biophysical Research Communications*, [online] 451(2), pp.314–318.
77. Yano, J.M., Yu, K., Donaldson, G.P., Shastri, G.G., Ann, P., Ma, L., Nagler, C.R., Ismagilov, R.F., Mazmanian, S.K., and Hsiao, E.Y., 2015. Indigenous bacteria from the gut microbiota regulate host serotonin biosynthesis. *Cell*, [online] 161(2), pp.264–276.